

UCSF

UC San Francisco Electronic Theses and Dissertations

Title

B cell peripheral tolerance is promoted by cathepsin B protease

Permalink

<https://escholarship.org/uc/item/0hc7q8sx>

Author

Chou, Marissa Yin

Publication Date

2023

Peer reviewed|Thesis/dissertation

B cell peripheral tolerance is promoted by cathepsin B protease

by
Marissa Chou

DISSERTATION
Submitted in partial satisfaction of the requirements for degree of
DOCTOR OF PHILOSOPHY

in

Biomedical Sciences

in the

GRADUATE DIVISION
of the
UNIVERSITY OF CALIFORNIA, SAN FRANCISCO

Approved:

DocuSigned by:

JULIE ZIKHERMAN

JULIE ZIKHERMAN

D967968925C2437...

Chair

DocuSigned by:

Anthony DeFranco

Anthony DeFranco

DocuSigned by:

Jason Cyster

Jason Cyster

5FFFC327038A40D...

Committee Members

To my parents, Dan Yu and James Chou, my sister Emily, my brother Byron,
and my grandparents, Li Hongren and Yu Qingfu—for their unconditional love and support.

ACKNOWLEDGEMENTS

This work was made possible by the support and encouragement of many, many individuals. First and foremost, I would like to thank my PhD advisor, Dr. Jason Cyster. Jason's reputation as a rigorous scientist and deep critical thinker precedes him, but being able to benefit firsthand from his mentorship—especially during our weekly meetings diving into the details of each experiment, considering all the potential controls, and rigorously analyzing results—has been invaluable to my scientific training. It is also impressive how dedicated and available Jason is to his trainees—be it personally helping us wean mice, making time to meet at a moment's notice, or sending edits for written material within impossibly fast turnaround times. I am forever grateful for all the opportunities afforded me in Jason's lab. The lessons I have learned from Jason in critical thinking and dedicated mentorship will undoubtedly shape my future career.

Thank you also to my thesis committee, Dr. Julie Zikherman and Dr. Anthony DeFranco. They have been indispensable in providing support and encouragement, both scientific and personal. I am grateful for their critical feedback in many productive discussions that helped further my progress at key points in my project. Julie has also been a wonderful mentor and role model to me in the physician-scientist training path; I cannot thank her enough. I would also like to thank several other faculty members who have contributed to my development and growth as an immunologist: my rotation mentors, Dr. Ari Molofsky and Dr. Mark Ansel, and the other members of my qualifying exam committee, Dr. Clifford Lowell and Dr. Lewis Lanier. I entered UCSF with very little immunology research experience, and it is truly a privilege to have been trained by these renowned giants in their fields.

I would be remiss to not mention the scientific mentors who shaped my interest in research and in pursuing this endeavor. My very first research experience was guided by Dr.

Christina Quigley in Dr. Jason (Xi) Jiang's lab. I am so lucky to have been taught the fundamentals of scientific practice by such patient, dedicated mentors who made science truly fun. This California girl would never have pursued this dual degree path if not for the spark ignited in Ohio. Immense thanks to Dr. Daniel Portnoy for providing me with my most impactful undergraduate research experience, and Dr. Chen Chen for being one of my most supportive champions. Working with them taught me how to be an independent, fearless, and creative scientist. Thank you also to Dr. Inna Vainshtein and Dr. Jackie Cheng at MedImmune, and Dr. Andy (Xiaodong) Huang and Dr. Mingjian Fei at Genentech for the opportunities that showed me translational arms of scientific research and were formative in shaping my decision to pursue this career path.

The day-to-day experience of my PhD would not have been the same without my fellow Cyster lab members. Dr. Michelle Mintz mentored me during my rotation, and the excitement and energy she brings to her science is truly infectious. It was an honor to work with her on the CD40L piece of her HVEM-BTLA story, and I am so lucky to have her as a mentor, role model, and friend. I would also like to thank Dr. Dan Liu for being another beacon in the lab. She has been my go-to person for discussing scientific ideas, troubleshooting experiments, locating reagents, and late-night boba deliveries. She never fails to amaze and inspire me with her persistence, resilience, and work ethic. Thank you to the many talented post-docs who have provided helpful discussions, feedback, and advice: Dr. Brian Laidlaw, Dr. Hsin Chen, Dr. Tamar Ben-Shaan, Dr. Marco DeGiovanni, Dr. Lihui Duan, Dr. Finn Wolfreys, Dr. Jessica Kotov, Dr. Ben Winer, Dr. Jianxuan Wu, Dr. Jianhang Yin, Dr. Zachary Earley, Dr. Konrad Knopper, and Dr. Fanglue Peng. Special thanks to Jinping An and Ying Xu for their priceless help with mouse lines, cloning, and library preparations. Thank you also to Hanna Taglinao for

brightening up the lab and keeping it in order, to Kenna Fowler and Viviana Davila for handling our lab operations, and to Bernarda Lopez for keeping our experiments running. Thank you to the LARC staff, especially Karla Mendoza, for her diligent care of our precious mice. Last, but certainly not least, thank you to the fellow graduate students for ensuring there is never a dull moment in lab: Dr. Erick Lu, Hanson Tam, Kevin Chen, and, in particular, my main baymates Dr. Antonia Gallman and Dr. Elise Wolf. Thank you for being there for me and sharing in all the successes and (much more numerous) failures that make up the emotional roller coaster of graduate school.

I would also like to thank members of the MSTP, BMS program, ImmunoX, and School of Medicine, whose leadership, wisdom, and guidance have been pillars of support throughout this prolonged training path: Dr. Mark Anderson, Dr. Aimee Kao, Dr. Mark Ansel, Dr. Anita Sil, Geri Ehle, Dr. Tiffani Quan, Demian Sainz, Andrés Zepeda, Jonathon Wilson, Ned Molyneaux, Amanda Andonian, Dennis Chan, Hallen Chung, and Valerie Margol.

Thank you to the many additional communities who have provided mentorship, support, and companionship. I am fortunate to be part of the best MSTP class with Abrar Choudhury, Fabian Fernandez, Sravani Kondapavulur, Elizabeth McCarthy, Cody Mowery, Marci Rosenberg, Iowis Zhu, and Lawrence Zhu. Though the journey is long, it has been made all the more meaningful with these friends by my side. Our MSTP immunology vertical mentoring group has blossomed over the years, providing a healthy mix of advice and gossip over boba. In particular, thank you to Theodore Roth for fearlessly leading our group, to my big siblings Ian Boothby and Antonia Gallman, and to my little sibling Irek Habrylo. Additionally, the incredibly nurturing community of the MSTP Women's Group has been a haven in navigating this path. Thank you to Parinaz Fozouni and Lay Kodama for championing this group; despite the many

amazing mentors we have, you two are my biggest role models. Thank you to my CMC group, led by Dr. Steve Polevoi: Celia Haering, Sophia Hernandez, Nhi Ho, and Edward Kempton—we are an unlikely group to band together, but it has been a privilege to learn alongside you. Thank you also to Didi Zhu and Priscila Muñoz Sandoval for sharing reagents, grad school memes, and food adventures with me. To those who have co-habitated with me over the years—Shirley Zhao, Joy Hsu, David Su, Ian Boothby, and Ricardo Guajardo—it has truly been a blessing to come home to such close friends at the end of long days (or nights) in lab and to share laughs over good food, TV shows, and board games; thank you.

Those who know me know how important my friends are to me. Words cannot express how grateful I am for the support you have given me in this journey, be it through food, music, ridiculous texts, or heartfelt conversations: Ishita Arora, Gregory Barber, Will Berdanier, Alexander Chao, Martin Consunji, Michael Deng, Ken Ferry, Giang Ha, Sophia Hernandez, Joy Hsu, Michelle Huang, Robert Huang, Kevin Huynh, Emily Jang, Sherman Jia, Abhi Kalakuntla, Sarah Kho, Lay Kodama, Briton Lee, Justine Leichtling, Kun Leng, Patricia Li, Wendy Liang, Reshena Liao, James Lim, Vivian Look, Amy Min, Iris Otani, Sanjana Parikh, Helen Pun, Zoya Qureshy, Matthew Schwede, David Su, Lakshmi Subbaraj, Abbie Wang, Cindy Wang, Prescott Watson, Andrew Wong, Andrew and Vivian Yousef, Shirley Zhao, and Jacqueline Zhu.

Thank you to my partner, Kevin Tse, for his unwavering love, patience, and belief in me throughout this process. Thank you for keeping my snacks stocked, keeping me well-fed, and keeping me company on the phone during late nights in lab. I have drawn on your endless support to renew my strength and motivation so many times throughout the course of this degree.

Last, but certainly not least, thank you to my family. My sister, Emily Chou, has always paved the way for me, and I thank her for keeping me humble and grounded. She is the most

reliable dessert partner, and I am fortunate to have her as a confidante, sister, and friend. Though he's technically younger, my brother, Byron Chou, has somehow surpassed and lapped me on the medical training racetrack. ("It's a race! I'm winning!") Despite all the challenges of his own career path, he always has a sunny outlook and disposition. ("It is lovely weather we are having.") I would like to thank him and Victoria Chen for all the food, recipes, gifts, and laughs we've shared. And finally to my parents—thank you for your unconditional love and support in all my endeavors, for your sacrifices to provide me with the best opportunities, and for all the times you've taken on burdens and hardships without a second thought just to make my life a little easier; 谢谢。

CONTRIBUTIONS TO PRESENTED WORK

The work described in this dissertation was done under the direct supervision of Dr. Jason Cyster, PhD. Chapters 2 and 3 are adapted from a publication under review at *Proceedings of the National Academy of Sciences*, “B cell peripheral tolerance is promoted by cathepsin B protease.” The thesis abstract was adapted from this work. The co-authors for this publication were Dan Liu, Jinping An, Ying Xu, and Jason G. Cyster. Dr. Cyster and I conceptualized the study, designed the experiments, interpreted the results, and collaboratively wrote the manuscript. I performed the experiments and prepared figures for publication. Dr. Dan Liu provided intellectual input and helped perform experiments. Ying Xu assisted with RNA sequencing library preparation and vector cloning. Jinping An genotyped mice.

B cell peripheral tolerance is promoted by cathepsin B protease

Marissa Yin Chou

ABSTRACT

B cells that bind soluble autoantigens receive chronic signaling via the B cell receptor (signal-1) in the absence of strong costimulatory signals (signal-2), and this leads to their elimination in peripheral tissues. The factors determining the extent of soluble autoantigen-binding B cell elimination are not fully understood. Here we demonstrate that elimination of B cells chronically exposed to signal-1 is promoted by cathepsin B (Ctsb). Using hen egg lysozyme- (HEL) specific immunoglobulin transgenic (MD4) B cells and mice harboring circulating HEL, we found improved survival and increased proliferation of HEL-binding B cells in Ctsb-deficient mice. Bone marrow (BM) chimera experiments established that both hematopoietic and non-hematopoietic sources of Ctsb were sufficient to promote peripheral B cell deletion. Depletion of CD4⁺ T cells overcame the survival and growth advantage provided by Ctsb deficiency, as did blocking CD40L or removing CD40 from the chronically antigen-engaged B cells. Thus, we suggest that Ctsb acts extracellularly to reduce soluble autoantigen-binding B cell survival and that its actions restrain CD40L-dependent pro-survival effects. These findings identify a role for cell-extrinsic protease activity in establishing a peripheral self-tolerance checkpoint.

TABLE OF CONTENTS

CHAPTER 1: Introduction	1
Mechanisms of B cell tolerance	2
Lessons in peripheral B cell tolerance via a model system	6
Cathepsin B and extracellular protease activity	7
References	9
CHAPTER 2: B cell peripheral tolerance is promoted by cathepsin B protease	16
Significance Statement	17
Abstract	18
Introduction	19
Results	21
Cathepsin B-deficient mice have normal follicles but reduced elimination of HEL-binding B cells.....	21
Cathepsin B from hematopoietic and non-hematopoietic cells promotes peripheral B cell tolerance	25
Follicular exclusion is intact in the absence of cathepsin B	26
CD4 ⁺ T cell depletion overcomes the effect of cathepsin B-deficiency on HEL-binding B cells.....	26
Enhanced HEL-binding B cell persistence in cathepsin B-deficient hosts depends on CD40L and CD40.....	29
Supplementary Figures	33
Materials and Methods	38
Mice	38

Cathepsin B activity assay	38
Adoptive transfer of MD4 B cells	39
HEL and antibody treatments	39
HEL serum measurements	40
Bone marrow chimeras	40
Immunizations	40
Immunofluorescence	41
Quantification of immunofluorescence images	42
Cell culture	42
Real-time PCR analysis	43
Flow cytometry	43
BAFF staining	44
Statistical analyses	44
Acknowledgements and Data Availability	44
CHAPTER 3: Conclusions	45
Conclusions	46
REFERENCES	50

LIST OF FIGURES

CHAPTER 1: Introduction

Figure 1.1	3
Figure 1.2	5

CHAPTER 2: B cell peripheral tolerance is promoted by cathepsin B protease

Figure 2.1	22
Figure 2.2	27
Figure 2.3	28
Figure 2.4	30
Supplementary Figure 2.1	34
Supplementary Figure 2.2	35
Supplementary Figure 2.3	37

CHAPTER 3: Conclusions

Figure 3.1	47
------------------	----

CHAPTER 1

Introduction

Mechanisms of B cell tolerance

B cells play a crucial role in humoral immune responses by generating high-affinity antibodies against a wide variety of foreign pathogens. However, the processes that allow for the recognition of such a vast range of antigens also lead to the production of self-reactive B cells, which must be restrained to prevent inappropriate B cell activation and thus the development of autoimmune disease (1, 2). It is estimated 50 – 70% of newly generated B cells are autoreactive (3, 4); thus, in order to prevent the inappropriate activation of autoreactive B cells, several checkpoint mechanisms operate in both the bone marrow and periphery to establish central and peripheral tolerance, respectively.

B cells develop in the bone marrow (BM) and generate their B cell receptors (BCRs) through the process of V(D)J recombination, which assembles unique BCRs from separate variable (V), diversity (D), and joining (J) gene segments. The combinatorial nature of this process allows for the incredible diversity of antigen receptors—at least 10^{12} possible unique permutations (5; 6). Inevitably, a portion of the BCRs generated by this stochastic process will be self-reactive. In the BM, BCR engagement with a self-antigen that causes strong receptor cross-linking and thus intracellular signaling results in receptor editing, whereby the BCR light chain can undergo further rearrangement (1, 7). If this edited BCR is still strongly self-reactive, the offending B cell undergoes cell death, otherwise known as clonal deletion (**Fig. 1.1**). This is a result of the regulation of many signaling inputs, such as increased levels of B cell linker protein (BLNK), Bruton's tyrosine kinase (Btk), and phospholipase (PLC) $\gamma 2$ (8), as well as the increase in pro-apoptotic factors, such as Bcl-2-interacting mediator of cell death (BIM) (1, 7, 9, 10).

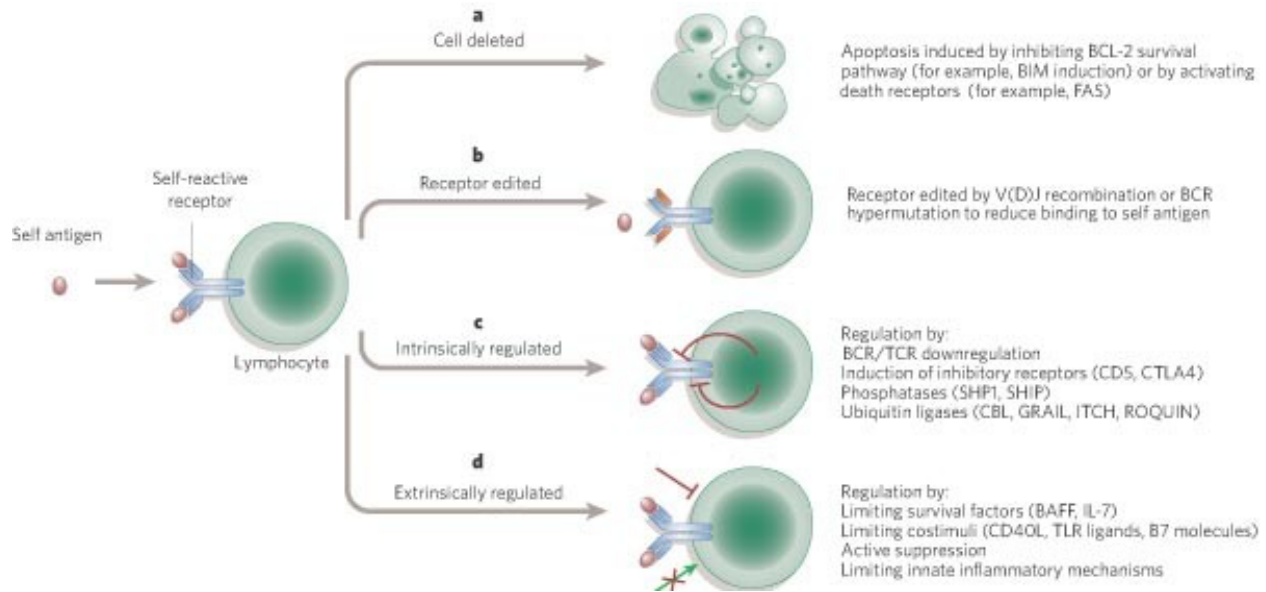


Figure 1.1 Goodnow, *et. al.* 2005 ***Tolerance mechanisms used to regulate self-reactive receptors.*** Mechanisms of clonal deletion (a), receptor editing (b), and signaling regulation (c, d) in self-reactive B cells.

B cells that are more weakly self-reactive are able to escape the aforementioned central tolerance mechanisms in the BM and migrate to secondary lymphoid organs. In the periphery, the two-signal model of lymphocyte activation posits that B cells that sense antigen via their BCR (signal-1) but do not receive co-stimulatory help (signal-2) from cognate T cells or pathogen-associated molecular patterns (PAMPs) are pushed to a less reactive state called anergy. Rather than being deleted, these B cells persist in the periphery but have reduced lifespans, altered migration and localization features, and are unable to mount functional antibody responses (11). While different anergic mouse models show varying phenotypes, anergic B cells generally display IgM downregulation, impaired BCR signaling (reduced Ig α , Ig β , and Syk phosphorylation), increased intracellular calcium due to chronic NFAT signaling and impaired calcium mobilization, failure to upregulate CD86 and CD80, and reduced proliferation (11). Interestingly, anergy is not a terminal state. Work using the Ars/A1 transgenic

mouse model showed that B cells that are no longer exposed to chronic signaling from their self-antigen can regain responsiveness (12).

One key aspect of anergic B cells is the negative regulation of BCR signaling, which includes a wide variety of downstream signaling molecules (**Figure 1.2**). Lyn, the primary BCR-associated Src-family kinase, has both positive and negative roles in BCR signaling. It has been shown to have important roles in recruiting inhibitory phosphatases, as well as inhibitory co-receptors. Both Lyn-deficient mice and mice constitutively expressing Lyn develop autoimmunity, demonstrating the importance of Lyn in regulating B cell anergy (13, 14). Additionally, the proximal arm of the BCR signaling cascade is actively restrained via inhibitory signaling molecules. In particular, the role of the inhibitory phosphatase SHP-1, encoded by the gene *Ptpn6*, has been well-studied in the context of autoimmunity. The *motheaten* (*me/me*) and *viable motheaten* (*me^v/me^v*) mutant mice, which contain mutations in *Ptpn6*, have widespread immune defects, including defects in B cell tolerance (15–18). A more recent study that generated a B cell-specific deletion of SHP1 observed an increase in B-1a cells, elevated serum immunoglobulin titers, and development of systemic autoimmunity (19).

Inhibitory phosphatases, such as SHP-1, but also SHP-2, SHIP-1, and SHIP-2, are recruited to the vicinity of the BCR by inhibitory co-receptors, such as CD22, CD72, and CD31, via their immunoreceptor tyrosine-based inhibitory motifs (ITIMs). Binding of the BCR to self-antigen results in phosphorylation of ITIM tyrosines by Src family kinases (SFK), which engages inhibitory phosphatases and thereby dampens activation of self-reactive B cells. ITIM-containing co-receptors have been shown to contribute to mechanisms of B cell development, B1 cell homeostasis, and modulation of tonic BCR signaling (2). For example, CD22 plays a critical role in regulating proximal BCR signaling responses, as CD22-deficient B cells show increased

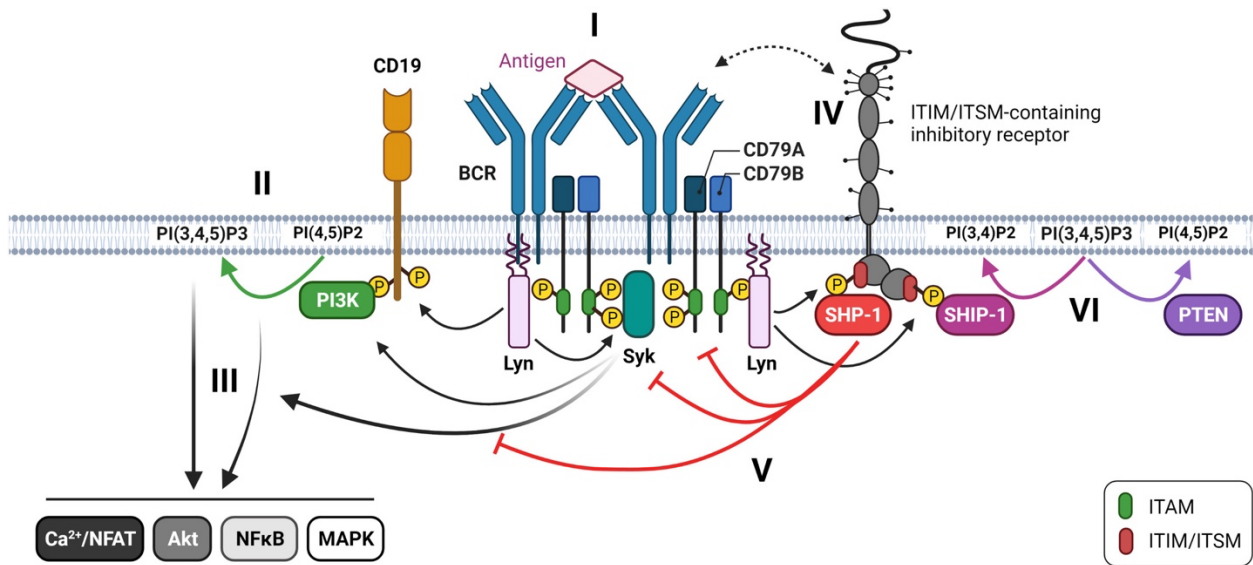


Figure 1.2 Getahun, et. al. 2022 **Regulation of BCR signaling.** Mechanisms of proximal BCR signaling: (I) BCR cross-linking by antigen binding, (II) activation of PI3K by Lyn and Syk, (III) intracellular signaling cascade, (IV) co-localization of ITIM/ITSM-containing receptors to the BCR, (V) inhibition of proximal signaling events by SHP-1, (VI) inhibition of PI3K signaling by SHIP-1 and PTEN.

phosphorylation of BCR-regulated molecules, such as BLNK, as well as enhanced calcium signaling (20–26). Similarly, CD72-deficient B cells have been shown to be hyperresponsive and hyperproliferative to BCR ligation, with enhanced signal transduction occurring in multiple pathways, such as NFAT, NFkB, and ERK (27, 28). Mice deficient in CD72 develop lupus-like disease by 6 months of age (29).

Further downstream, additional phosphatases, such as PTEN and SHIP-1, are increased in anergic B cells and act to suppress the PI3K pathway. Studies have shown that deletion of PTEN or SHIP-1 results in a loss of anergy; and moreover, haploinsufficiency of both phosphatases does, as well, illustrating the importance of the PI3K pathway in maintaining anergy and tolerance (14). Altogether, the diversity of molecules involved in the regulation of B cell

signaling and maintenance of anergy highlights the many layers of regulation that restrain B cell activation to prevent autoantibody production and autoimmune disease development.

Lessons in peripheral B cell tolerance via a model system

The immunoglobulin (Ig) transgenic mouse line (called MD4) has been a widely used model for studying B cell tolerance. These mice harbor an immunoglobulin transgene specific for hen egg lysozyme (HEL). A separate transgenic mouse line called ML5 expresses soluble HEL as a neoself-antigen under the metallothionein promoter, which facilitates HEL expression from embryonic to adult life (30). In ML5 mice, serum HEL levels are in the 20 – 50 ng/mL range (30, 31). These two lines were also intercrossed to generate a double transgenic line whereby all the B cells are chronically exposed to HEL “autoantigen,” resulting in a B cell repertoire with reduced surface IgM levels (though normal IgD) (30). Studies placing these HEL-engaged B cells into a competitive wild-type (WT) polyclonal environment showed that they were excluded from the B cell follicles, partially due to reduced CXCR5 levels, and deleted within three days (31–34). One mechanism of this deletion or competitive elimination of HEL-engaged B cells is due to their augmented dependence on the limited pro-survival factor B-cell activating factor (BAFF) (35). Soluble HEL is poor at promoting T cell responses in B6 mice (36, 37), and T cells in the HEL-expressing ML5 mouse model developed tolerance, most likely due to the presence of HEL in the thymus, thus causing negative selection of HEL-specific T cells (30). Yet, in the setting of T cell deficiency, HEL-engaged B cells are further eliminated, suggesting non-cognate naïve CD4⁺ T cell help can contribute to the survival of chronically antigen-engaged B cells (31, 33). Freshly isolated naïve CD4⁺ T cells do not display detectable surface CD40L, likely due to downmodulation by CD40-induced endocytosis, shedding, or blocking by soluble CD40 (38, 39). However, it has been found that naïve CD4⁺ T cells

constitutively express CD40L, which can be measured on the cell surface when CD40 is removed (40). Thus, naïve CD4⁺ T cells may provide a source of non-cognate help, or signal-2, for autoantigen-engaged B cells.

Cathepsin B and extracellular protease activity

Cell-cell interactions rely on the dynamic nature of the cell surface, which is constantly being remodeled. Cysteine proteases are one of the four major classes of proteases, along with serine proteases, aspartic proteases, and metalloproteases, and are involved in numerous cell surface functions, including antigen processing, extracellular matrix turnover, and surface protein processing (41, 42). Of the cysteine proteases, cathepsins (whose name is derived from the Greek *kathesein*, meaning “to digest”) are the most abundant family (42). Cathepsin B is ubiquitously expressed and synthesized as a preprocathepsin in the endoplasmic reticulum (ER). Shortly thereafter, the N-terminal signal peptide directs the preprocathepsin form of cathepsin B to the ER lumen where it is cleaved into its procathepsin form (41). It is then trafficked to endosomes or lysosomes, where the acidic pH enables autoactivation into active cathepsin B. In the lysosome, cathepsin B has been shown to degrade various hormones and growth factors, such as perilipin (PLIN) 1, increasing lipolysis in adipose tissue (43); the MCOLN1/TRPML1 calcium channel to inhibit autophagy and regulate lysosomal biogenesis (44); and key Alzheimer’s proteins, including amyloid- β and the amyloid precursor protein (APP) (45, 46). Cytosolic cathepsin B has also been reported to induce degradation of the pro-apoptotic protein Bid (47) and receptor-interacting protein 1 (Rip1) kinase to limit macrophage necroptosis (48).

More recently, the extracellular role of cathepsins has been appreciated. One mechanism of cathepsin secretion is via lysosomal exocytosis, which can be induced by immunomodulatory

states, such as inflammatory cytokine signaling or cancer. Cathepsin B has been shown to be released by lysosomal exocytosis, as well as deposited on the plasma membrane caveolae (49, 50). Though cathepsins require acidic pH for activation and optimal activity, the less active procathepsin form is stable at neutral pH. Many niches, such as the bone lacunae (51), foster a local acidic microenvironment to facilitate cathepsin function, or certain inflammatory states may also promote acidification, as is the case in the tumor microenvironment.

In the extracellular environment, cathepsin B has been reported to perform several functions. One study described the role of secreted extracellular cathepsin B from microglia in mediating neuronal cell death (52). Other reported functions, largely based on *in vitro* studies, include extracellular matrix proteolysis (53), protecting against self-killing by cytotoxic CD8⁺ T cells (54), TGF β activation (55), generation of soluble TRAIL (56), and chemokine cleavage (57). One study showed extracellular cathepsin B to be required for the cleavage and solubilization of CXCL13, an important B cell chemokine. This enzymatic step was suggested to be key in allowing CXCL13 to establish the gradient necessary to form B cell follicles in secondary lymphoid tissues. However, it was not shown that cathepsin B performs this cleavage of CXCL13 *in vivo* (58). Given the diversity of suggested targets for cathepsin B, it is reasonable to speculate that this protease and, perhaps, other extracellular cathepsins have roles in regulating cellular interactions and cell fates in the immune system.

REFERENCES

1. C. C. Goodnow, J. Sprent, B. Fazekas de St Groth, C. G. Vinuesa, Cellular and genetic mechanisms of self tolerance and autoimmunity. *Nature* **435**, 590-597 (2005).
2. T. Tsubata, B-cell tolerance and autoimmunity. *F1000Res* **6**, 391 (2017).
3. H. Wardemann, S. Yurasov, A. Schaefer, J. W. Young, E. Meffre, M. C. Nussenzweig, Predominant autoantibody production by early human B cell precursors. *Science* **301**, 1374-1377 (2003).
4. D. Nemazee, Antigen receptor 'capacity' and the sensitivity of self-tolerance. *Immunol. Today* **17**, 25-29 (1996).
5. J. G. Cyster and C. D. C. Allen, B cell responses: cell interaction dynamics and decisions. *Cell* **177**, 524-540 (2019).
6. B. Briney, A. Inderbitzin, C. Joyce, D. R. Burton, Commonality despite exceptional diversity in the baseline human antibody repertoire. *Nature* **566**, 393-397 (2019).
7. D. Nemazee, Mechanisms of central tolerance for B cells. *Nature Rev. Immunol.* **17**, 281-294 (2017).
8. R. J. Benschop, E. Brandl, A. C. Chan, J. C. Cambier, Unique signaling properties of B cell antigen receptors in mature and immature B cells: implications for tolerance and activation. *J. Immunol.* **167**, 4172-4179 (2001).
9. P. Bouillet *et al.*, Proapoptotic Bcl-2 relative Bim required for certain apoptotic responses, leukocyte homeostasis, and to preclude autoimmunity. *Science* **286**, 1735-1738 (1999).

10. A. Enders, P. Bouillet, H. Puthalakath, Y. Xu, D. M. Tarlinton, A. Strasser, Loss of the pro-apoptotic BH3-only Bcl-2 family member Bim inhibits BCR stimulation-induced apoptosis and deletion of autoreactive B cells. *J. Exp. Med.* **198**, 1119-1126 (2003).
11. J. C. Cambier, S. B. Gauld, K. T. Merrell, B. J. Vilen, B-cell anergy: from transgenic models to naturally occurring anergic B cells? *Nat. Rev. Immunol.* **7**, 633-643 (2007).
12. A. Getahun, Role of inhibitory signaling in peripheral B cell tolerance. *Immunol. Rev.* **307**, 27-42 (2022).
13. M. L. Hibbs *et al.*, Sustained activation of Lyn tyrosine kinase in vivo leads to autoimmunity. *J. Exp. Med.* **196**, 1593-1604 (2022).
14. S. E. Franks and J. C. Cambier, Putting on the brakes: regulatory kinases and phosphatases maintaining B cell anergy. *Front. Immunol.* **9** (2018).
15. M. C. Green and L. D. Shultz, Motheaten, an immunodeficient mutant of the mouse: I. Genetics and pathology. *Journal of Heredity* **66**, 250-258 (1975).
16. L. D. Schultz and M. C. Green, Motheaten, an immunodeficient mutant of the mouse. *J. Immunol.* **116**, 936 (1976).
17. L. D. Shultz, D. R. Coman, C. L. Bailey, W. G. Beamer, C. L. Sidman, 'Viable motheaten,' a new allele at the motheaten locus. I. Pathology. *Am. J. Pathol.* **116**, 179–192 (1984).
18. J. G. Cyster and C. C. Goodnow, Protein tyrosine phosphatase 1C negatively regulates antigen receptor signaling in B lymphocytes and determines thresholds for negative selection. *Immunity* **2**, 13–24 (1995).
19. L. I. Pao *et al.*, B cell-specific deletion of protein-tyrosine phosphatase Shp1 promotes B-1a cell development and causes systemic autoimmunity. *Immunity* **27**, 35–48 (2007).

20. L. Nitschke, CD22 and Siglec-G: B-cell inhibitory receptors with distinct functions. *Immunol Rev* **230**, 128–143 (2009).
21. S. J. Meyer, A. T. Linder, C. Brandl, L. Nitschke, B cell siglecs—News on signaling and its interplay with ligand binding. *Front. Immunol.* **9**, 2820 (2018).
22. L. Nitschke, R. Carsetti, B. Ocker, G. Köhler, M. C. Lamers, CD22 is a negative regulator of B-cell receptor signalling. *Current Biology* **7**, 133–143 (1997).
23. T. L. O’Keefe, G. T. Williams, S. L. Davies, M. S. Neuberger, Hyperresponsive B cells in CD22-deficient mice. *Science* **274**, 798 (1996).
24. K. L. Otipoby *et al.* CD22 regulates thymus-independent responses and the lifespan of B cells. *Nature* **384**, 634–637 (1996).
25. S. Sato *et al.* CD22 is both a positive and negative regulator of B lymphocyte antigen receptor signal transduction: Altered signaling in CD22-deficient mice. *Immunity* **5**, 551–562 (1996).
26. J. Gerlach *et al.* B cell defects in SLP65/BLNK-deficient mice can be partially corrected by the absence of CD22, an inhibitory coreceptor for BCR signaling. *Eur. J. Immunol.* **33**, 3418–3426 (2003).
27. D. H. Li *et al.* CD72 down-modulates BCR-induced signal transduction and diminishes survival in primary mature B lymphocytes. *J. Immunol.* **176**, 5321 (2006).
28. D. H. Li *et al.* Modulation of peripheral B cell tolerance by CD72 in a murine model. *Arthritis Rheum.* **58**, 3192–3204 (2008).
29. M. Xu *et al.* Cd72(c) is a modifier gene that regulates Fas(lpr)-induced autoimmune disease. *J. Immunol.* **190**, 5436 (2013).

30. C. C. Goodnow *et al.* Altered immunoglobulin expression and functional silencing of self-reactive B lymphocytes in transgenic mice. *Nature* **334**, 676-682 (1988).
31. K. N. Schmidt and J. G. Cyster, Follicular exclusion and rapid elimination of hen egg lysozyme autoantigen-binding B cells are dependent on competitor B cells, but not on T cells. *J. Immunol.* **162**, 284-291 (1999).
32. J. G. Cyster, S. B. Hartley, C. C. Goodnow, Competition for follicular niches excludes self-reactive cells from the recirculating B-cell repertoire. *Nature* **371**, 389-395 (1994).
33. J. G. Cyster and C. C. Goodnow, Antigen-induced exclusion from follicles and anergy are separate and complementary processes that influence peripheral B cell fate. *Immunity* **3**, 691-701 (1995).
34. E. H. Ekland, R. Forster, M. Lipp, J. G. Cyster, Requirements for follicular exclusion and competitive elimination of autoantigen-binding cells. *J. Immunol.* **172**, 4700-4708 (2004).
35. R. Lesley *et al.*, Reduced competitiveness of autoantigen-engaged B cells due to increased dependence on BAFF. *Immunity* **20**, 441-453 (2004).
36. G. Gammon *et al.* The choice of T-cell epitopes utilized on a protein antigen depends on multiple factors distant from, as well as at the determinant site. *Immunol. Rev.* **98**, 54-73 (1987).
37. Y. S. Jang, J. A. Mikszta, B. S. Kim, T cell epitope recognition involved in the low-responsiveness to a region of hen egg lysozyme (46-61) in C57BL/6 mice. *Molecular Immunology* **31**, 803-812 (1994).
38. Y. Koguchi, T. J. Thauland, M. K. Slifka, D. C. Parker, Preformed CD40 ligand exists in secretory lysosomes in effector and memory CD4⁺ T cells and is quickly expressed on the cell surface in an antigen-specific manner. *Blood* **110**, 2520-2527 (2007).

39. J. L. Gardell and D. C. Parker, CD40L is transferred to antigen-presenting B cells during delivery of T-cell help. *Eur. J. Immunol.* **47**, 41-50 (2017).
40. R. Lesley, M. Kelly, Y. Xu, J. G. Cyster, Naïve CD4 T cells constitutively express CD40L and augment autoreactive B cell survival. *Proc. Natl. Acad. Sci. U. S. A.* **103**, 10717-10722 (2006).
41. T. Yadati, T. Houben, A. Bitorina, R. Shiri-Sverdlov, The ins and outs of cathepsins: Physiological function and role in disease management. *Cells* **9**, 1679 (2020).
42. S. Verma, R. Dixit, K. C. Pandey, Cysteine proteases: Modes of activation and future prospects as pharmacological targets. *Front. Pharmacol.* **7**, 1-26 (2016).
43. J. Kovsan, R. Ben-Romano, S. C. Souza, A. S. Greenberg, A. Rudich, Regulation of adipocyte lipolysis by degradation of the perilipin protein: nelfinavir enhances lysosome-mediated perilipin proteolysis. *J. Biol. Chem.* **282**, 21704-21711 (2007).
44. S. M. Man and T. D. Kanneganti, Regulation of lysosomal dynamics and autophagy by CTSB/cathepsin B. *Autophagy* **12**, 2504-2505 (2016).
45. S. Cermak *et al.* Loss of cathepsin B and L leads to lysosomal dysfunction, NPC-like cholesterol sequestration and accumulation of the key Alzheimer's proteins. *PLoS One* **11**, e0167428 (2016).
46. C. Wang, B. Sun, Y. Zhou, A. Grubb, L. Gan, Cathepsin B degrades amyloid- β in mice expressing wild-type human amyloid precursor protein. *J. Biol. Chem.* **287**, 39834-39841 (2012).
47. G. Droga-Mazovec *et al.* Cysteine cathepsins trigger caspase-dependent cell death through cleavage of bid and antiapoptotic Bcl-2 homologues. *J. Biol. Chem.* **283**, 19140-19150 (2008).

48. S. McComb, B. Shutinoski, S. Thurston, E. Cessford, K. Kumar, S. Sad, Cathepsins limit macrophage necroptosis through cleavage of Rip1 kinase. *J. Immunol.* **192**, 5671-5678 (2014).
49. T. Castro-Gomes, M. Corrotte, C. Tam, N. W. Andrews, Plasma membrane repair is regulated extracellularly by proteases released from lysosomes. *PLoS One* **11**, e0152583 (2016).
50. D. T. Jane, L. Morvay, L. Dasilva, D. Cavallo-Medved, B. F. Sloane, M. J. Dufresne, Cathepsin B localizes to plasma membrane caveolae of differentiating myoblasts and is secreted in an active form at physiological pH. *Biol. Chem.* **387**, 223-234 (2006).
51. D. Q. Yang, S. Feng, W. Chen, H. Zhao, C. Paulson, Y. P. Li, V-ATPase subunit ATP6AP1 (Ac45) regulates osteoclast differentiation, extracellular acidification, lysosomal trafficking, and protease exocytosis in osteoclast-mediated bone resorption. *J. Bone Miner. Res.* **27**, 1695-1707 (2012).
52. L. Gan *et al.* Identification of cathepsin B as a mediator of neuronal death induced by A β -activated microglial cells using a functional genomics approach. *J. Biol. Chem.* **279**, 5565-5572 (2004).
53. K. Porter, Y. Lin, P. B. Liton, Cathepsin B is up-regulated and mediates extracellular matrix degradation in trabecular meshwork cells following phagocytic challenge. *PLoS One* **8**, e68668 (2013).
54. K. N. Balaji, N. Schaschke, W. Machleidt, M. Catalfamo, P. A. Henkart, Surface cathepsin B protects cytotoxic lymphocytes from self-destruction after degranulation. *J. Exp. Med.* **196**, 493-503 (2002).

55. M. Guo, P. A. Mathieu, B. Linebaugh, B. F. Sloane, J. J. Reiners, Jr., Phorbol ester activation of a proteolytic cascade capable of activating latent transforming growth factor-betaL a process initiated by the exocytosis of cathepsin B. *J. Biol. Chem.* **277**, 14829-14837 (2002).
56. S. M. Mariani, P. H. Krammer, Differential regulation of TRAIL and CD95 ligand in transformed cells of the T and B lymphocyte lineage. *Eur. J. Immunol.* **28**, 973-982 (1998).
57. L. Hasan *et al.*, Function of liver activation-regulated chemokine/CC chemokine ligand 20 is differently affected by cathepsin B and cathepsin D processing. *J. Immunol.* **176**, 6512-6522 (2006).
58. J. Cosgrove *et al.*, B cell zone reticular cell microenvironments shape CXCL13 gradient formation. *Nature Communications* **11**, 3677 (2020).

CHAPTER 2

B cell peripheral tolerance is promoted by cathepsin B protease

SIGNIFICANCE STATEMENT

Self-tolerance in the B cell compartment of soluble autoantigens depends on mechanisms that promote peripheral B cell elimination. In this study we report that deficiency in the cysteine protease cathepsin B (Ctsb) in mice results in less efficient removal of chronically antigen-engaged B cells from the repertoire. The tolerogenic action of Ctsb is lost in mice lacking the CD40 pathway, and the findings suggest that Ctsb restrains, directly or indirectly, basal CD40L-CD40 pathway activity and thereby helps prevent activation of autoreactive B cells. Since protease activity is increased at sites of inflammation, our findings point to the possibility that self-tolerance checkpoints are reset in these sites due to proteolytic modulation of cell surface interaction molecules.

ABSTRACT

B cells that bind soluble autoantigens receive chronic signaling via the B cell receptor (signal-1) in the absence of strong costimulatory signals (signal-2), and this leads to their elimination in peripheral tissues. The factors determining the extent of soluble autoantigen-binding B cell elimination are not fully understood. Here we demonstrate that elimination of B cells chronically exposed to signal-1 is promoted by cathepsin B (Ctsb). Using hen egg lysozyme- (HEL) specific immunoglobulin transgenic (MD4) B cells and mice harboring circulating HEL, we found improved survival and increased proliferation of HEL-binding B cells in Ctsb-deficient mice. Bone marrow chimera experiments established that both hematopoietic and non-hematopoietic sources of Ctsb were sufficient to promote peripheral B cell deletion. Depletion of CD4 T cells overcame the survival and growth advantage provided by Ctsb deficiency, as did blocking CD40L or removing CD40 from the chronically antigen-engaged B cells. Thus, we suggest that Ctsb acts extracellularly to reduce soluble autoantigen-binding B cell survival and that its actions restrain CD40L-dependent pro-survival effects. These findings identify a role for cell-extrinsic protease activity in establishing a peripheral self-tolerance checkpoint.

INTRODUCTION

Self-tolerance in the B cell compartment is established through multiple checkpoints (1). Antigens that strongly cross-link the B cell receptor (BCR) on developing B cells in the bone marrow (BM) cause receptor editing or deletion. B cells that recognize low valency soluble autoantigens are not held up at the immature B cell checkpoint but are instead regulated by peripheral checkpoints. One model that has been widely used to study tolerance induction in response to soluble autoantigen involves immunoglobulin (Ig) transgenic mice (called MD4) that are specific for hen egg lysozyme (HEL) and transgenic mice that express soluble HEL as a neoself-antigen (called ML5) (2). In double transgenic mice generated by intercrossing these two lines, the B cells are all autoantigen-engaged and thus chronically receiving B cell receptor (BCR) signals (signal-1). These HEL-binding B cells are not receiving cognate T cell help or being exposed to pathogen-associated molecular patterns (PAMPS) and thus are not receiving signal-2. HEL-engaged B cells have reduced surface IgM levels and a reduced ability to signal in vitro in response to exogenous HEL. When these chronically HEL-engaged B cells are placed in the polyclonal repertoire of wild-type (WT) mice, they undergo follicular exclusion and are deleted from the periphery within a few days (3, 4). This competitive elimination of B cells receiving chronic signal-1 without signal-2 occurs in part due to an increased dependence of the cells on the pro-survival factor BAFF and the limited availability of this factor in mice with a polyclonal B cell repertoire (5, 6). As well as being strongly dependent on BAFF, survival of B cells receiving chronic signal-1 in the absence of signal-2 was augmented by naïve CD4 T cells (7). Although naïve CD4 T cells are not conventionally considered to be a source of CD40L (and thus signal-2), our previous work showed that naïve CD4 T cells constitutively express CD40L though it is not measurable on the cell surface due to continual modulation by engagement with

CD40-expressing cells; when these cells are removed, surface CD40L can be detected (8).

Whether additional extrinsic factors beyond BAFF and naïve CD4 T cell CD40L influence the survival of peripheral B cells chronically exposed to signal-1 is unclear.

Cathepsin B (Ctsb) is a widely expressed member of the cysteine cathepsin family (9). It is expressed as a proenzyme in the endoplasmic reticulum, and it becomes a mature protease in the lysosome. It carries out a variety of functions in the lysosome such as processing other lysosomal enzymes and mediating degradation of hormones (9, 10). Ctsb is also found in multiple extracellular locations. Extracellular functions attributed to Ctsb include proteolysis of the extracellular matrix (11), protection of cytotoxic T cells from self-killing (12), generation of soluble TRAIL (TNFSF10) (13), TGF β activation (14), and cleavage of several chemokines (15). In some cases, the extracellular function was thought to occur while Ctsb was associated with the surface of the secreting cell (10). Of particular relevance to B cell biology, a recent study suggested that extracellular Ctsb was required for cleavage of CXCL13 to help establish a gradient of this chemokine for organization of B cell follicles in lymphoid tissues (16).

Here we set out to further characterize the influence of Ctsb on B cell follicle organization and function. In the Ctsb-deficient mice studied here, we did not observe a defect in follicular organization. However, when MD4 B cells were transferred into Ctsb-deficient mice containing soluble HEL such that they experienced chronic signal-1, the extent of B cell deletion was reduced compared to transfers into matched WT mice. Our experiments establish that hematopoietic and non-hematopoietic cells both contribute to the production of Ctsb that promotes HEL-binding B cell elimination. The effect of Ctsb on HEL-binding B cells was overcome in mice depleted of CD4 T cells or deficient in CD40L function or in CD40. These findings suggest a pathway by which extracellular protease activity promotes B cell tolerance.

RESULTS

Ctsb-deficient mice have normal follicles but reduced elimination of HEL-binding B cells

Follicular organization in *Ctsb*-deficient mice was examined by staining spleen and lymph node sections for B cell and follicular dendritic cell (FDC) markers. Since the prior study had reported a requirement for *Ctsb* to maintain primary follicles and FDCs (16), we examined unimmunized mice. In the *Ctsb*^{-/-} mouse colony studied here, lymphoid follicle organization in spleen and lymph nodes was intact and FDCs were readily detected (**Supplementary Fig. 2.1A and Supplementary Fig. 2.1B**). Analysis of *Ctsb* activity in spleen interstitial fluid using an enzyme activity assay confirmed the *Ctsb*-deficiency (**Fig. 2.1A**). These data suggest *Ctsb* is not essential for establishing the CXCL13 activity needed for follicular organization.

We next considered whether *Ctsb* might influence the fate of different types of follicular B cells. *Ctsb*-deficient mice had normal frequencies of splenic B cells and CD4⁺ T cells and slightly reduced CD8⁺ T cells (**Supplementary Fig. 2.1C**) as previously reported (16). The mice mounted intact splenic germinal center (GC) responses to sheep red blood cells (SRBCs), a model T-dependent antigen (**Supplementary Fig. 2.1D**). The chronic GC responses present in mesenteric lymph nodes and Peyer's patches were also comparable between *Ctsb*-deficient and control mice (**Supplementary Fig. 2.1E**). Since the naïve and GC B cell compartments appeared intact, we next asked whether the fate of B cells experiencing chronic signal-1 was affected. This was tested in *Ctsb*-deficient mice by taking advantage of the finding that when mice harboring low frequencies of MD4 B cells are injected with large amounts of soluble HEL, the HEL-binding B cells experience chronic BCR engagement and are deleted within three days (7). This outcome is analogous to the loss that occurs when MD4 B cells are transferred into ML5 mice that express HEL endogenously (4). Using this MD4 cell transfer and HEL injection approach,

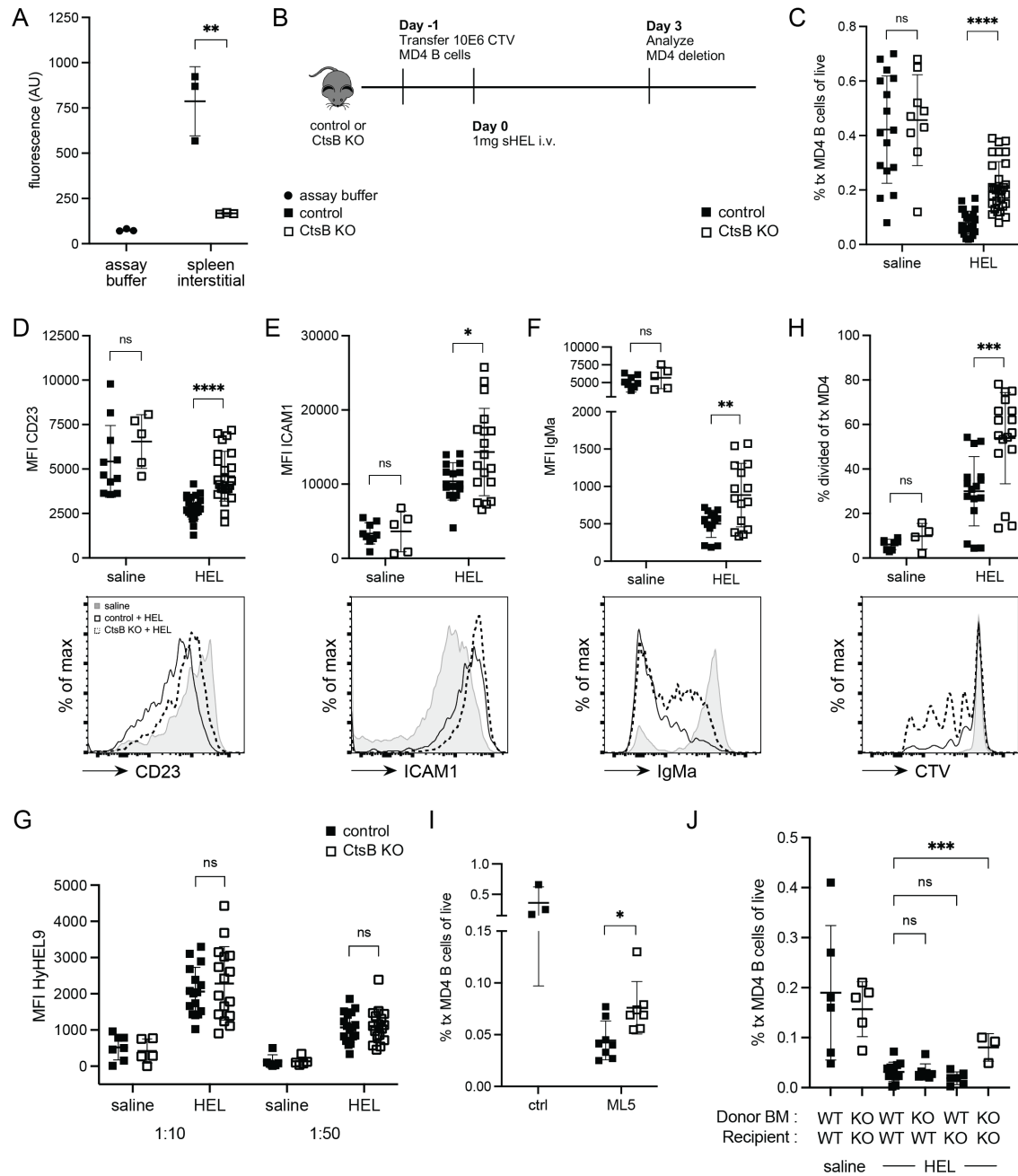


Figure 2.1. Cathepsin B promotes elimination of HEL-binding B cells.

(A) *Ctsb* activity in assay buffer or spleen interstitial fluid of control (*Ctsb*^{+/+} or *Ctsb*^{+/-}) or *Ctsb*^{-/-} (*CtsB* KO) mice. Data show results from two separate experiments. (B) Schematic of CTV-labeled MD4 B cell adoptive transfer into control or *Ctsb*-deficient mice, followed by HEL treatment. (C) Frequencies of transferred MD4 B cells in spleens of control or *Ctsb*-deficient recipients 3 days after saline (n = 16 control, n = 9 KO mice) or HEL treatment (n = 26 control, n = 30 KO mice). (D–F) MFI (top) and representative histogram plot (bottom) of CD23 (D), ICAM1 (E), and IgM^a (F) on transferred MD4 B cells 3 days after saline (n = 11 control, n = 5 KO) or HEL treatment (n = 22 control, n = 24 KO). (G) MFI of HyHEL9 on MD4 B cells incubated with 1:10 or 1:50 dilutions of sera from control or *Ctsb*-deficient mice 3 days after

saline (n = 7 control, n = 5 KO) or HEL treatment (n = 16 control, n = 17 KO). (H) Percentage of divided transferred MD4 B cells (top) or representative histogram plot of CTV (bottom) 3 days after saline (n = 8 control, n = 4 KO) or HEL treatment (n = 16 control, n = 17 KO). (I) Frequencies of transferred MD4 B cells in spleens of control ML5⁺ (n = 8) or Ctsb-deficient ML5⁺ (n = 7) recipients 3 days after MD4 B cell adoptive transfer. Control ML5⁻ (n = 3) mice used as deletion control. (J) Frequencies of transferred MD4 B cells in spleens of bone marrow (BM) chimeras 3 days after saline or HEL treatment. The Ctsb genotype of donor BM and recipient mice used to generate the BM chimeras is indicated. In graphs, each data point indicates an individual mouse and lines indicate means. Error bars represent SDs. I is representative of three experiments. Statistical significance for A–I was determined by unpaired t test. NS, not significant; *P < 0.05; **P < 0.01; ***P < 0.001; ****P < 0.0001. Statistical significance for J was determined by ordinary one-way ANOVA, ***, P=0.0007.

we observed the expected marked elimination of splenic HEL-binding B cells in control recipients (**Fig. 2.1B** and **Fig. 2.1C**). However, the extent of deletion was significantly reduced in *Ctsb*-deficient mice (**Fig. 2.1C**). Similar findings were made in peripheral lymph nodes (**Supplementary Fig. 2.2A**). Analysis of the surface phenotype of the transferred cells showed higher CD23 and ICAM1 levels on HEL-binding B cells in the *Ctsb*-deficient recipients (**Fig. 2.1D** and **Fig. 2.1E**). The reduced expression of CD23 on HEL-engaged B cells is consistent with the ability of BCR signaling to downmodulate this marker (17). Surface IgM was also present at higher levels on a fraction of the HEL-binding B cells in *Ctsb*-deficient recipients (**Fig. 2.1F**). Since IgM downmodulation is highly sensitive to the extent of HEL exposure, we examined serum HEL abundance in the treated control and *Ctsb*-deficient mice. This was done by incubating MD4 B cells with serum taken from control and *Ctsb*-deficient mice at day 3 after HEL injection and then staining with HyHEL9 to detect the amount of bound HEL. Control and *Ctsb*-deficient mouse serum contained comparable amounts of HEL (**Fig. 2.1G**) thereby excluding differences in HEL availability as an explanation for the improved survival of HEL-binding B cells in mice lacking *Ctsb*. Using cell trace violet (CTV) labeling to track cell division in the transferred cells, few cells divided in control recipients as expected, but there was an increase in cell division in *Ctsb*-deficient recipients (**Fig. 2.1H**). Assessment of the frequencies of divided and undivided B cells showed that both were increased (**Fig. 2.1H** and **Supplementary Fig. 2.2B**), indicating that *Ctsb*-deficiency augmented both proliferation and survival of B cells experiencing chronic BCR signaling. Analysis of the surface marker phenotype in divided and undivided transferred B cells showed a greater difference among the divided B cells, suggesting the mechanism promoting proliferation also contributed to the increased CD23, ICAM1, and IgM (**Supplementary Fig. 2.2C–E**).

To confirm that the HEL injection approach was an accurate model for events occurring during autoantigen exposure, we crossed *Ctsb*^{-/-} mice with ML5 mice. Transferred MD4 cells were mostly deleted within 3 days of transfer into control ML5 mice, but the deletion was reduced in *Ctsb*^{-/-} ML5 mice (**Fig. 2.1I**). Serum HEL concentrations in ML5 mice were unchanged by *Ctsb* deficiency (**Supplementary Fig. 2.2F**). The HEL-binding B cells in *Ctsb*-deficient ML5 mice showed elevated CD23, ICAM1 and IgM (**Supplementary Fig. 2.2G–I**). The fraction of cells that divided was also increased (**Supplementary Fig. 2.2J**). Thus, *Ctsb* contributes to restraining HEL-autoantigen binding B cell activation and to promoting their removal from the peripheral B cell repertoire.

To test for possible effects of *Ctsb* on BAFF abundance, we took advantage of the finding that the BAFF availability is reflected in the amount that is bound to receptors on the B cell surface (5). Using a polyclonal anti-BAFF serum, the amount of surface BAFF on B cells from control and *Ctsb*-deficient mice was equivalent (**Supplementary Fig. 2.3A**). As the size of the B cell compartment is highly responsive to BAFF availability (18), the unchanged size of the B cell compartment in *Ctsb*-deficient mice (**Supplementary Fig. 2.1C**) provided further evidence that BAFF abundance was not altered by *Ctsb* deficiency.

***Ctsb* from hematopoietic and non-hematopoietic cells promotes peripheral B cell tolerance**

Our transfer studies utilized WT MD4 B cells and thus established that the action of *Ctsb* in promoting elimination of B cells receiving chronic signal-1 was cell-extrinsic. To determine whether *Ctsb* was needed in hematopoietic or non-hematopoietic cells, we generated WT → *Ctsb* KO, *Ctsb* KO → WT and *Ctsb* KO → *Ctsb* KO BM chimeras. After 7-8 weeks reconstitution MD4 B cells were transferred and soluble HEL injected. Deletion efficiency was intact in all the

chimeras except the Ctsb KO -> Ctsb KO group (**Fig. 2.1J**). These data indicate that Ctsb from either hematopoietic cells or radiation-resistant (most likely non-hematopoietic stromal) cells was sufficient for promoting elimination of HEL-binding B cells.

Follicular exclusion is intact in the absence of Ctsb

To test whether follicular exclusion of HEL-binding B cells was impaired in the absence of Ctsb, spleens were taken from WT and Ctsb KO mice that harbored MD4 B cells and had been treated with soluble HEL one day earlier. Imaging analysis revealed the MD4 B cells were predominantly located at the follicle T-zone interface in both WT and Ctsb-deficient recipients (**Fig. 2.2A–C**). Transferred MD4 B cells were equally distributed in the follicle, as determined by IgD⁺ staining, in saline-treated WT and Ctsb-deficient mice (data not shown). Thus, Ctsb is not required for follicular exclusion of antigen-engaged B cells.

CD4⁺ T cell depletion overcomes the effect of Ctsb-deficiency on HEL-binding B cells

Since prior work had established that naïve CD4⁺ T cells restrained the extent of HEL-binding B cell elimination in WT mice (7), we tested whether the action of Ctsb was influenced by CD4⁺ T cells. Control and Ctsb KO mice were treated with a CD4⁺ T cell depleting antibody and then used as recipients of MD4 cells and soluble HEL (**Fig. 2.3A**). In contrast to the findings in control treated recipients, there was a similar extent of deletion in control and Ctsb-deficient mice when CD4⁺ T cells were lacking (**Fig. 2.3B**). There was also a loss in the increased levels of CD23, ICAM1 and IgM (**Fig. 2.3C–E**). The effect of Ctsb-deficiency on HEL-binding B cell proliferation was also lost in CD4⁺ T cell depleted mice (**Fig. 2.3F**). These data suggest that the B cell deletion-promoting effect of Ctsb may involve restraining some

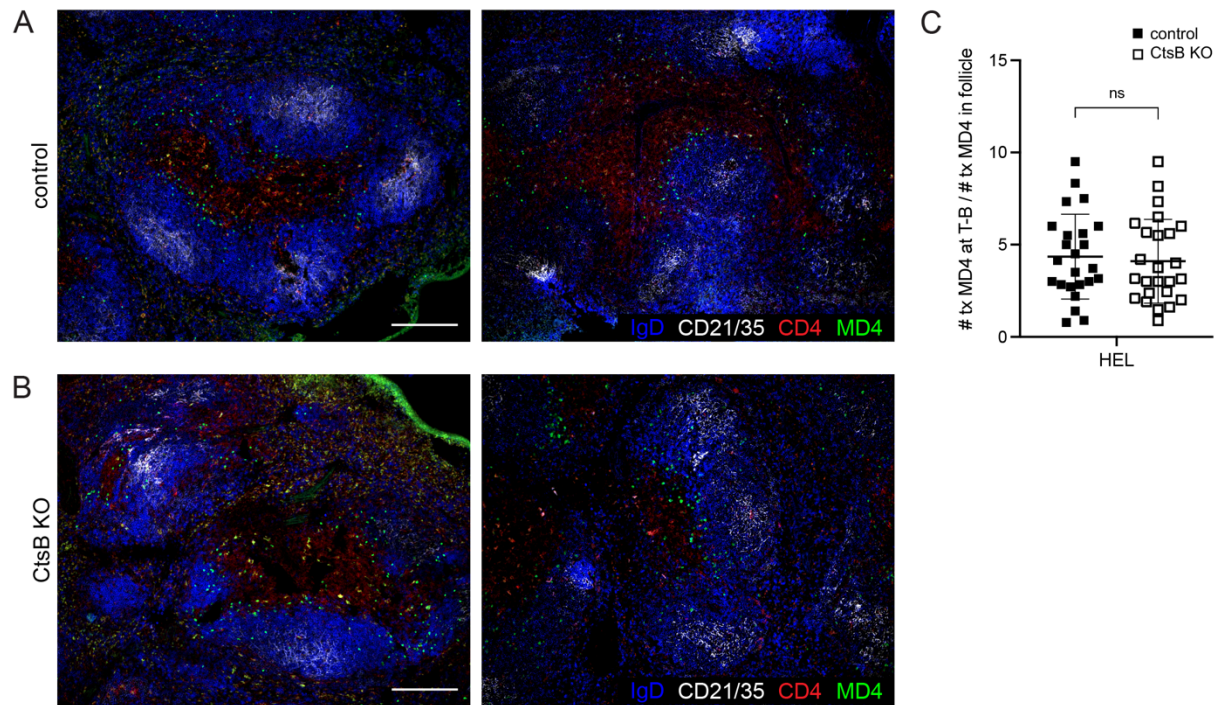


Figure 2.2. Follicular exclusion of HEL-engaged B cells is unaffected by cathepsin B deficiency.

(A, B) Immunofluorescence for MD4 GFP B cells (GFP, green) transferred into HEL-treated control (A) or *Ctsb*-deficient (B) mice stained to detect endogenous B cell follicles (IgD, blue; CD21/35, white) and the T cell zone (CD4, red). Sections were prepared one day after HEL treatment. Two example images are shown and are representative of multiple cross sections from at least three mice of each type. Scale bar, 200 μ m. (C) Quantification of proportion of MD4 GFP B cells at the T zone – follicle (T-B) interface one day after HEL treatment. Each data point represents an individual follicle (n = 24 control, n = 25 KO) from sections prepared from at least 3 individual mice of each genotype. Lines indicate means, and error bars represent SDs. Statistical significance for C was determined by unpaired t test. NS, not significant.

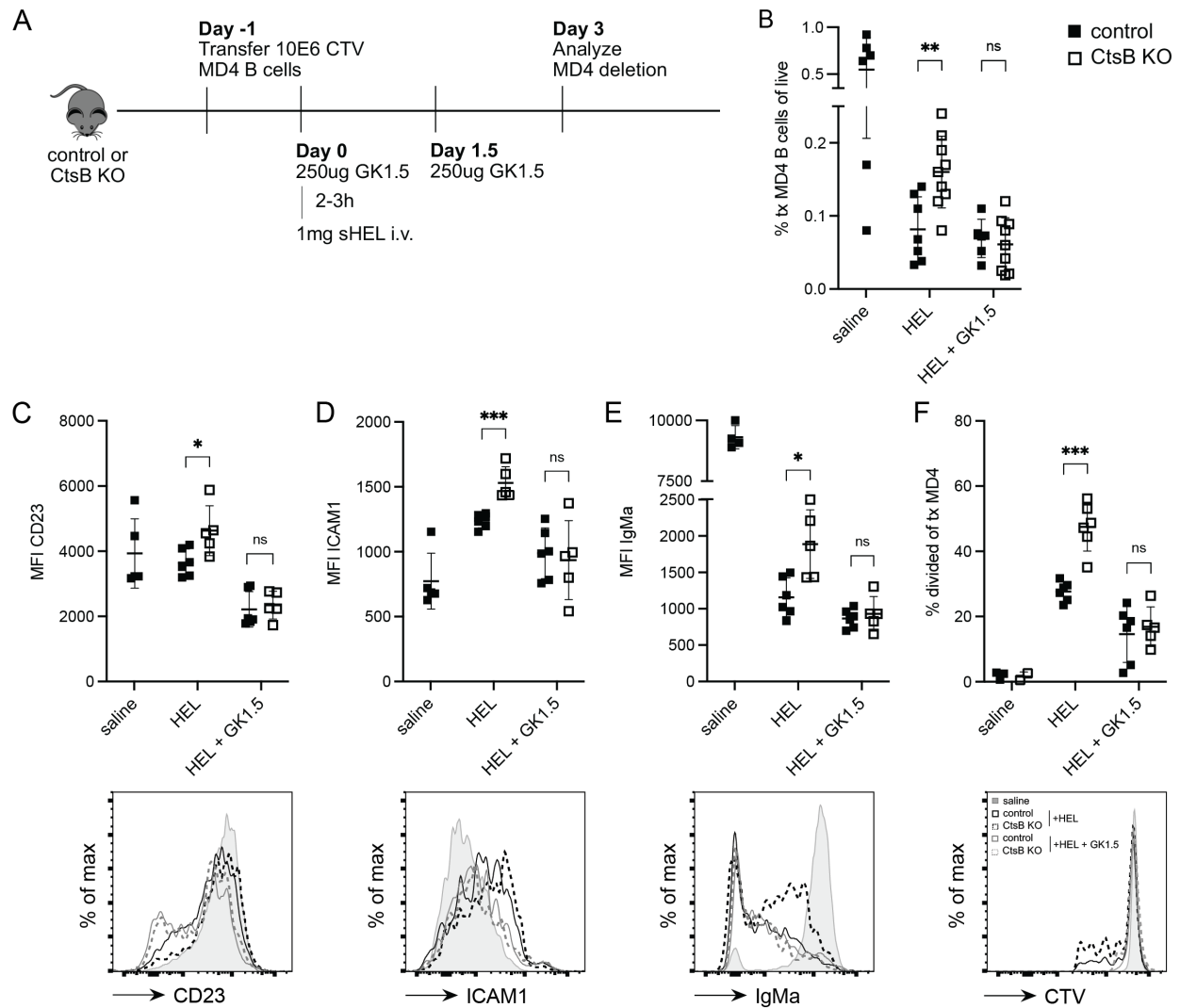


Figure 2.3. Depletion of CD4 T cells overcomes the effect of cathepsin B deficiency on HEL-binding B cells.

(A) Schematic of CTV-labeled MD4 B cell adoptive transfer into control or *Ctsb*-deficient mice, followed by GK1.5 CD4⁺ T cell depletion and HEL treatment. (B) Frequencies of transferred MD4 B cells in spleens of control or *Ctsb*-deficient recipients 3 days after saline (n = 6 control), HEL (n = 7 control, n = 9 KO), or HEL with GK1.5 treatment (n = 6 control, n = 9 KO). (C–E) MFI (top) and representative histogram plot (bottom) of CD23 (C), ICAM1 (D), and IgM^a (E) on transferred MD4 B cells 3 days after saline (n = 5 control), HEL (n = 6 control, n = 5 KO), or HEL with GK1.5 treatment (n = 6 control, n = 5 KO). (F) Percentage of divided transferred MD4 B cells (top) or representative histogram plot of CTV (bottom) 3 days after saline (n = 3 control, n = 2 KO), HEL (n = 6 control, n = 6 KO), or HEL with GK1.5 treatment (n = 6 control, n = 5 KO). Each data point indicates an individual mouse and lines indicate means. Error bars represent SDs. C–F are representative of three experiments. Statistical significance for B–F was determined by unpaired t test. NS, not significant; *P < 0.05; **P < 0.01, ***P < 0.001.

function of CD4⁺ T cells. Previous work had found that naïve CD4⁺ T cells can limit the extent of HEL autoantigen-binding B cell elimination through provision of CD40L (8). Therefore, we next examined the effect of CD40L blockade.

Enhanced HEL-binding B cell persistence in Ctsb-deficient hosts depends on CD40L and CD40

Control and Ctsb KO mice were treated with CD40L-blocking antibody, and the fate of MD4 B cells after HEL treatment was examined. Blocking CD40L had a similar effect to CD4⁺ T cell ablation, overcoming the effect of Ctsb-deficiency on HEL-binding B cell accumulation (**Fig. 2.4A**). This included a loss in CD23 and ICAM1 induction (**Fig. 2.4B** and **Fig. 2.4C**) and a complete loss of increased cell division (**Fig. 2.4D**). We then examined CD40L transcript levels in sorted naïve CD4⁺ T cells and found they were abundant as expected (8) and were unaltered by Ctsb deficiency (**Fig. 2.4E**). Moreover, surface CD40L on PMA plus ionomycin-activated control and Ctsb-deficient CD4⁺ T cells was equivalent (**Fig. 2.4F**). CD40 engagement of CD40L causes loss of CD40L from the T cell surface (19-21); however, when purified naïve CD4⁺ T cells are incubated in a low density culture and thus in the absence of CD40 exposure, CD40L becomes detectable on the cell surface (8). When control and Ctsb KO CD4⁺ T cells were incubated in this way the KO cells showed a trend for more surface display of CD40L, but this difference was not statistically significant (**Fig. 2.4G** and **Supplementary Fig. 2.3B**). Thus, under the conditions tested, Ctsb did not significantly alter CD40L expression. Finally, as a further test of the contribution of CD40L to the augmented survival of HEL-binding B cells in Ctsb-deficient hosts, we co-transferred WT and CD40^{-/-} MD4 B cells into control and Ctsb KO hosts and treated them with soluble HEL. Analysis 3 days later showed comparable deletion in

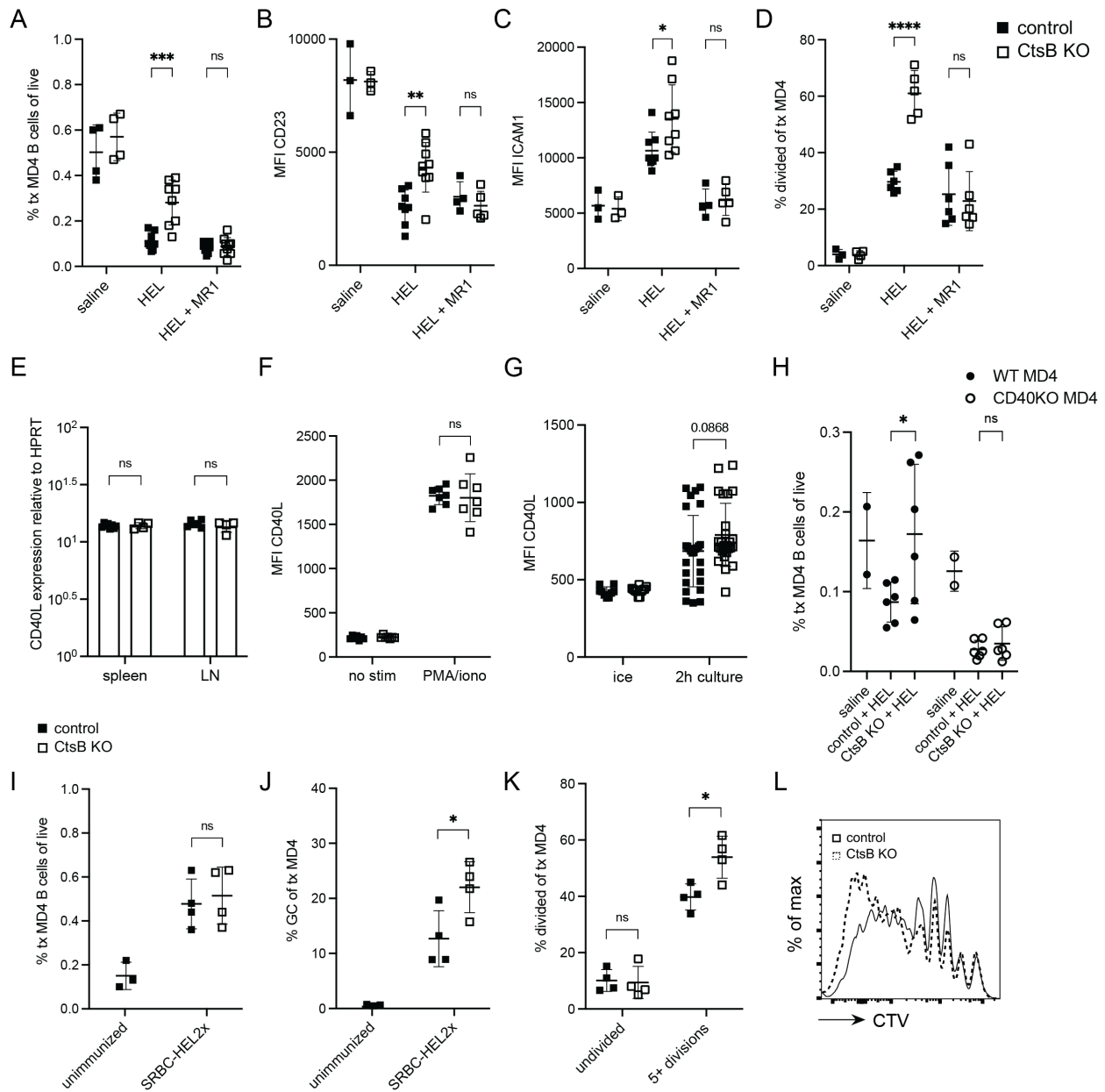


Figure 2.4. Enhanced HEL-binding B cell persistence in *Ctsb*-deficient hosts depends on CD40L and CD40.

(A) Frequencies of transferred MD4 B cells in spleens of control or *Ctsb*-deficient recipients 3 days after saline, HEL, or HEL with MR1 CD40L-blocking treatment. (B, C) MFI of CD23 (B) and ICAM1 (C) on transferred MD4 B cells 1.5 days after saline (n = 4 control, n = 4 KO), HEL (n = 8 control, n = 8 KO), or HEL with MR1 treatment (n = 9 control, n = 9 KO). (D) Percentage of divided transferred MD4 B cells 3 days after saline (n = 3 control, n = 4 KO), HEL (n = 6 control, n = 5 KO), or HEL with MR1 treatment (n = 6 control, n = 6 KO). (E) CD40L transcript abundance in naïve CD4⁺ T cells isolated from spleen and lymph node tissues harvested from control (n = 6) or *Ctsb*^{-/-} (n = 3) mice. CD40L and hypoxanthine phosphoribosyltransferase (HPRT) transcripts were quantitated by real-time PCR. Data show results from two separate

experiments. (F) MFI of CD40L on purified CD4⁺ T cells from control (n = 7) or *Ctsb*-deficient (n = 8) mice incubated without (no stim) or with (PMA/iono) PMA and ionomycin for 2 h at 37°C. (G) MFI of CD40L on purified CD4⁺ T cells from control (n = 27) or *Ctsb*-deficient (n = 26) mice kept on ice or incubated in a dilute culture for 2 h at 37°C. (H) Frequencies of WT or CD40-deficient MD4 B cells after 1:1 mixed transfer of CD45.1 WT and CD45.2 CD40-deficient MD4 B cells in spleens of control or *Ctsb*-deficient recipients 3 days after saline (n = 2 control, n = 2 KO) or HEL treatment (n = 6 control, n = 6 KO). (I, J) Frequencies of total (I) and germinal center (GC) B cells (J) of transferred MD4 cells in spleens of unimmunized mice (n = 3) or mice immunized with SRBC-HEL^{2x} (n = 4 control, n = 4 KO). (K) Frequencies of undivided MD4 B cells or MD4 B cells having undergone 5 or more divisions in spleens of control (n = 4) or *Ctsb*-deficient mice (n = 4) 5 days after SRBC-HEL^{2x} immunization. (L) Representative histogram plot of CTV labeling of transferred MD4 B cells 5 days after SRBC-HEL^{2x} immunization. Each data point indicates an individual mouse and lines indicate means. Error bars represent SDs. A–D and H are representative of three experiments. I–L are representative of two experiments. Statistical significance for A–K was determined by unpaired t test. NS, not significant; *P < 0.05; **P < 0.01; ***P < 0.001; ****P < 0.0001.

both types of recipients (**Fig. 2.4H**). CD40-deficiency also prevented elevation of ICAM1 and IgM though there was still some induction of CD23 (**Supplementary Fig. 2.3C** and **Supplementary Fig. 2.3D**). The expression of IgM was widely dispersed in this experiment (**Supplementary Fig. 2.3E**). CD40 abundance on WT MD4 B cells in control and *Ctsb*-deficient mice was similar (**Supplementary Fig. 2.3F**). Taken together, these data suggest that the effect of *Ctsb* on augmenting deletion of HEL-binding B cells involves a process that limits the CD40L-CD40 engagement that occurs when HEL-binding B cells encounter naïve CD4⁺ T cells in lymphoid tissues.

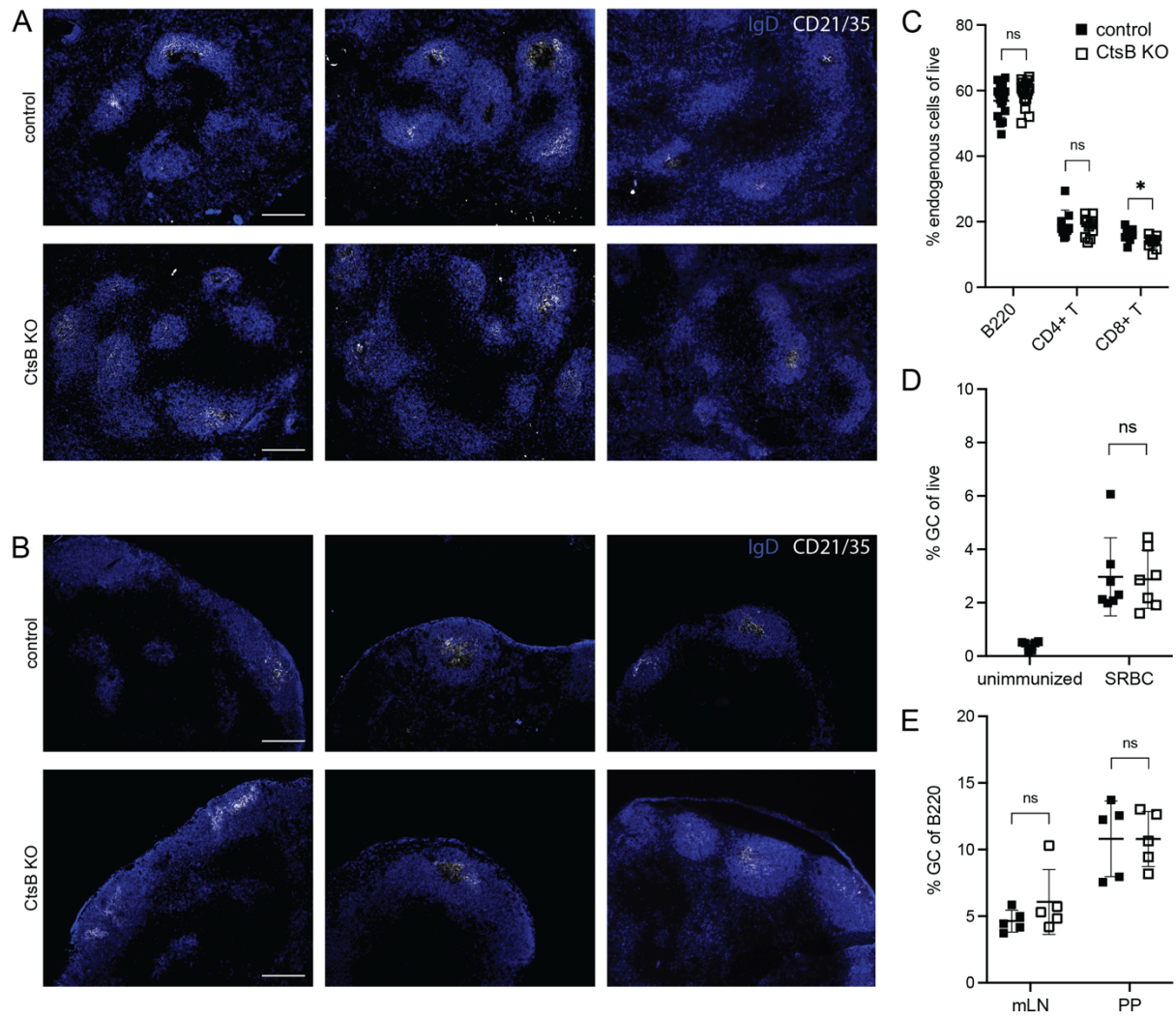
Although we did not observe an alteration in the polyclonal GC response to complex foreign or gut-associated antigens (**Supplementary Fig. 2.1D** and **Supplementary Fig. 2.1E**), our findings suggesting that non-cognate T-dependent signals could be increased in the absence of *Ctsb* led us to perform a further experiment examining cognate T cell help. We transferred MD4 cells into WT or *Ctsb*-deficient recipients and immunized the mice with HEL^{2x}, a form of HEL with reduced affinity for the MD4 BCR (22), coupled to strongly immunogenic SRBCs. Upon analysis at 5 days, although total numbers of MD4 B cells were similar between recipients, we observed an increase in the fraction of MD4 cells that had a GC phenotype in the immunized *Ctsb*-deficient compared to control recipients (**Fig. 2.4I** and **Fig. 2.4J**). Moreover, CTV dilution analysis showed that the MD4 cells had undergone more extensive cell division in the *Ctsb*-deficient recipients (**Fig. 2.4K** and **Fig. 2.4L**). These data indicate that under some conditions, *Ctsb* can restrain the extent of T cell help in response to foreign antigen.

SUPPLEMENTARY FIGURES

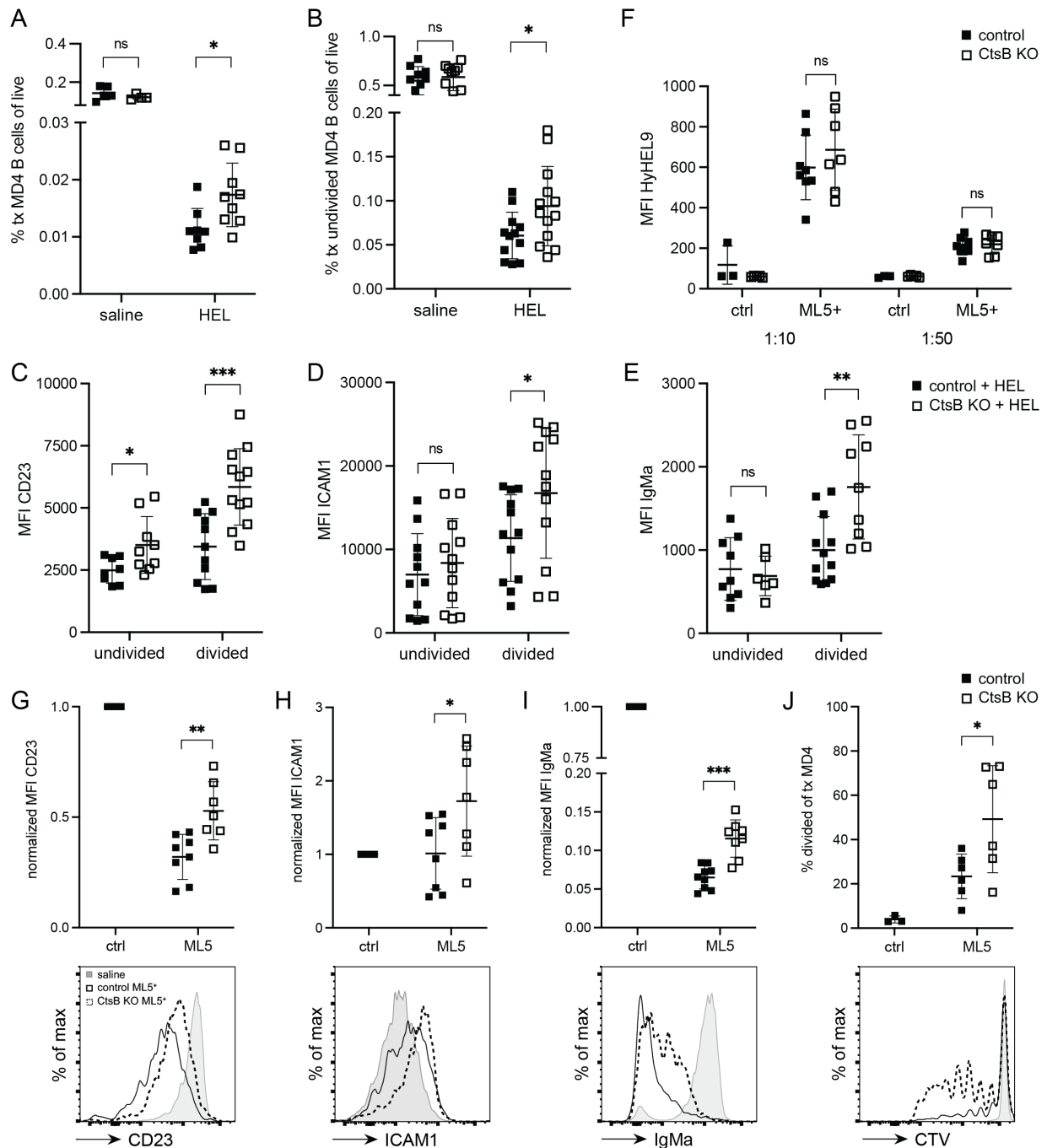
Supplementary Figure 2.1

Supplementary Figure 2.2

Supplementary Figure 2.3

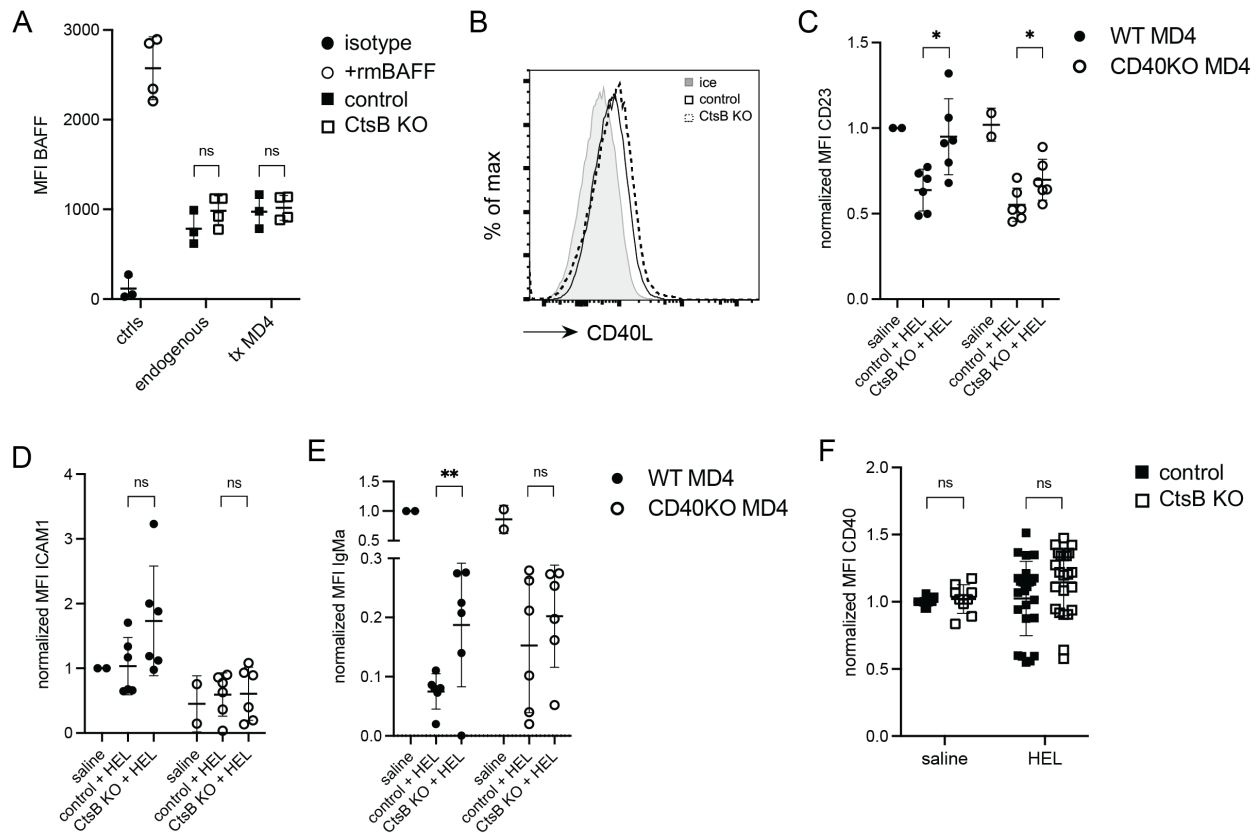


Supplementary Figure 2.1. (A, B) Immunofluorescence for B cell follicles (IgD, blue) and FDCs (CD21/35, white) in spleen (A) and peripheral lymph nodes (B) from control (Ctsb^{+/+} or Ctsb^{+/-}, top row) or Ctsb^{-/-} (bottom row) mice. Scale bar, 200 μ m. Three example images are shown and are representative of multiple cross sections from at least three mice of each type. (C) Frequencies of B, CD4⁺ T, and CD8⁺ T cells in spleens of control or Ctsb-deficient mice (N \geq 9 mice per genotype). (D) Frequencies of germinal center (GC) B cells in spleens of unimmunized mice (n = 6), or control (n = 7) or Ctsb-deficient (n = 7) mice 5 days after sheep red blood cell (SRBC) immunization. (E) Frequencies of GC B cells in mesenteric lymph nodes or Peyer's patches of control (n = 5) or Ctsb-deficient (n = 5) mice at homeostasis. Each data point indicates an individual mouse and lines indicate means. Error bars represent SDs. D is representative of three experiments. Statistical significance for C–E was determined by unpaired t test. NS, not significant; *P < 0.05.



Supplementary Figure 2.2. (A) Frequencies of transferred MD4 B cells in lymph nodes of control or Ctsb-deficient recipients 3 days after saline (n = 5 control, n = 4 KO mice) or HEL treatment (n = 8 control, n = 9 KO). (B) Frequencies of undivided (CTV-high) transferred MD4 B cells in spleens of control or Ctsb-deficient recipients 3 days after saline (n = 10 control, n = 10 KO) or HEL treatment (n = 12 control, n = 13 KO). (C–E) MFI of CD23 (C), ICAM1 (D), and IgM^a (E) on undivided and divided transferred MD4 B cells in control or Ctsb-deficient recipients 3 days after HEL treatment (N ≥ 6 mice per genotype). (F) MFI of HyHEL9 on MD4 B cells incubated with 1:10 or 1:50 dilutions of sera from control ML5⁻ (n = 3), Ctsb-deficient

ML5⁻ (n = 5), control ML5⁺ (n = 8), or Ctsb-deficient ML5⁺ (n = 7) mice. (G–I) Normalized MFI (top) and representative histogram plot (bottom) of CD23 (G), ICAM1 (H), and IgM^a (I) on transferred MD4 B cells in control ML5⁺ (n = 8) or Ctsb-deficient ML5⁺ (n = 7) mice 3 days after MD4 B cell adoptive transfer. Control ML5⁻ (n = 4) mice used as deletion control. (J) Percentage of divided transferred MD4 B cells (top) or representative histogram plot of CTV (bottom) in control ML5⁺ (n = 6) or Ctsb-deficient ML5⁺ (n = 6) mice 3 days after MD4 B cell adoptive transfer. Control ML5⁻ (n = 3) mice used as deletion control. Each data point indicates an individual mouse and lines indicate means. Error bars represent SDs. A and C–J are representative of three experiments. Statistical significance for A–J was determined by unpaired t test. NS, not significant; *P < 0.05; **P < 0.01.



Supplementary Figure 2.3. (A) MFI of anti-BAFF staining on endogenous B cells and transferred MD4 B cells at day 3 in control (n = 3) or Ctsb-deficient (n = 3) mice. Control column (ctrls) indicates staining with control antibody (isotype) or pre-incubation with 10 μ g/mL recombinant mouse BAFF (+rmBAFF) prior to anti-BAFF staining. (B) Representative histogram plot of CD40L on purified CD4⁺ T cells kept on ice or incubated in a dilute culture for 2 h at 37°C. (C–E) Normalized MFI of CD23 (C), ICAM1 (D), and IgM^a (E) on WT or CD40-deficient MD4 B cells from 1:1 mixed transfer of CD45.1 WT and CD45.2 CD40-deficient MD4 B cells in spleens of recipient mice 3 days after saline (n = 2 control, n = 2 KO) or HEL treatment (n = 6 control, n = 6 KO). (F) Normalized MFI of CD40 on transferred MD4 B cells 3 days after saline (n = 11 control, n = 9 KO) or HEL treatment (n = 24 control, n = 23 KO). Each data point indicates an individual mouse and lines indicate means. Error bars represent SDs. A and C–E are representative of three experiments. Statistical significance for A and C–F was determined by unpaired t test. NS, not significant; *P < 0.05; **P < 0.01.

MATERIALS AND METHODS

Mice

All mice were bred internally, and 6- to 20-week-old mice of both sexes were used. Cathepsin-deficient [B6;129-*Ctsb*^{tm1Jde}/J] mice were obtained from JAX and were backcrossed 6 times to C57BL/6J. CD40-deficient [B6.129P2-*Cd40*^{tm1Kik}/J] mice were obtained from JAX. MD4 mice [C57BL/6-Tg(IghelMD4)4Ccg/J] and UBC-GFP (Tg(UBC-GFP)30Scha/J) mice were from an internal colony. ML5 mice (Tg(ML5sHEL)5Ccg) were obtained from Julie Zikherman, University of California, San Francisco, CA. CD45.1 B6 (B6.SJL-PtprcaPepcb/BoyCrCr1) mice used for chimera recipients and cell transfer experiments were bred internally from founders ordered from JAX. In most experiments, littermates were used as controls and experimental animals were co-caged in groups of 2–6 whenever possible. All mice were analyzed between 8 and 20 wk of age. Animals were housed in a specific pathogen-free environment in the Laboratory Animal Research Center at UCSF, and all experiments conformed to ethical principles and guidelines approved by the UCSF Institutional Animal Care and Use Committee.

Cathepsin B Activity Assay

Spleens from WT and *Ctsb*^{-/-} mice were mashed through a 70 µm cell strainer in 700µL of PBS. Resulting cell suspensions were centrifuged at 1,500 rpm at 4°C to pellet cells. The interstitial fluid-containing supernatant (or “mashate”) was collected, diluted 1:10, and *Ctsb* activity was measured using a fluorometric *Ctsb* activity assay (Abcam).

Adoptive Transfer of MD4 B Cells

Spleens and lymph nodes from CD45.1 MD4 mice were macerated and resulting cell suspensions were filtered through a 70 μm mesh into PBS supplemented with 2% FCS and 1mM EDTA. Counting beads were used for the enumeration of cells, and frequency of MD4 B cells was determined by staining of IgM^a-positive B cells on the flow cytometer. Cells were labeled with Cell Trace Violet (CTV) (Invitrogen) and 5–10 $\times 10^6$ MD4 B cells were injected intravenously into recipient mice. For positioning of HEL-binding B cells, spleens and lymph nodes from CD45.1 MD4 GFP mice were prepared as above. MD4 B cells were enriched by negative selection using biotinylated antibodies against CD43, CD4, CD8, TCR β , CD11c, and Ter119, followed by streptavidin-conjugated beads (EasySep Streptavidin RapidSpheres) to greater than 95% purity. Counting beads were used for the enumeration of cells, and 5–10 $\times 10^6$ MD4 B cells were injected intravenously into recipient mice. For CD40-deficient MD4 experiments, CD45.1 WT MD4 and CD45.2 CD40^{-/-} MD4 spleens and lymph nodes were prepared as above. WT and CD40^{-/-} MD4 splenocytes were mixed such that the MD4 B cells reached a 1:1 ratio. Cells were labeled with CTV, and 10–15 $\times 10^6$ MD4 B cells were injected intravenously into recipient mice.

HEL and Antibody Treatments

Recipient mice were injected intravenously with 1 mg hen egg lysozyme (HEL) (Sigma) one day after adoptive transfer of MD4 B cells. For CD4⁺ T cell depletion experiments, 250 μg anti-mouse CD4 GK1.5 monoclonal antibody (BioXCell) was injected intravenously 2-3 h before HEL treatment on d0 and on d1.5. For CD40L blocking experiments, 250 μg anti-mouse CD40L MR1 monoclonal antibody (BioXCell) was injected intravenously on d0 and d1.5.

HEL Serum Measurements

Serum was collected from WT or *Ctsb*^{-/-} mice 3 days after 1 mg HEL treatment or from WT ML5⁺ or *Ctsb*^{-/-} ML5⁺ mice. MD4 B cells were plated in a 96-well plate at 5×10^6 cells per ml in PBS supplemented with 2% FCS and incubated with sera at 1:10 and 1:50 dilutions for 20 min on ice. Cells were washed 3 times and HEL occupancy was measured by staining with HyHEL9-PE-Cy5.5 (in house).

Bone Marrow Chimeras

CD45.1 B6 or *Ctsb*^{-/-} mice were lethally irradiated with 1,100 rads gamma irradiation (split dose separated by 3 hours) and then i.v. injected with relevant BM cells under isoflurane anesthesia. Chimeras were used as recipients for adoptive transfer experiments as described above after 8 to 10 weeks of reconstitution.

Immunizations

Recipient mice were immunized intravenously with 2×10^8 SRBC (Colorado Serum Company) in a volume of 200 μ L. Spleens were harvested on day 5. For SRBC-HEL^{2 \times} experiments, 1×10^5 MD4 B cells were CTV-labeled and transferred into recipient mice. The following day, mice were immunized intravenously with 2×10^8 SRBC-HEL^{2 \times} , and spleens were harvested on day 5 post-immunization. Conjugation of SRBC-HEL^{2 \times} was done as previously described (29). Briefly, SRBCs were first washed with PBS three times, mixed with 20 μ g/ml HEL^{2 \times} (Gift of R. Brink), crosslinked with 100 μ L of 100mg/mL EDCI (1-ethyl-3-(3-dimethylaminopropyl) carbodiimide) (Sigma-Aldrich) in conjugation buffer (0.35M mannitol and 0.01M NaCl in ddH₂O) for 30 min, and washed three times to remove the free HEL.

Immunofluorescence

Lymph nodes and spleens were embedded in optimal cutting temperature compound.

Cryosections of 7 μm were dried for 1 hour, fixed in acetone for 10 min, and dried for 1 hour at room temperature. Slides were rehydrated in PBS containing 0.1% fatty acid-free bovine serum albumin (BSA) for 10 min. A solution consisting of 1% normal mouse serum (NMS), 1% normal donkey serum (NDS), 1:100 AF647-conjugated anti-mouse CD21/35 (BD Bioscience, catalog no. 123424) and 1:300 goat anti-mouse IgD (Cedarlane Laboratories, GAM/IGD(FC)/7S) was used to label FDCs and endogenous naïve B cells, respectively. This solution was incubated with the slides overnight at 4°C. The slides were then washed in PBS and stained with AMCA-conjugated donkey anti-goat IgG (Jackson ImmunoResearch, 705-156-147) at room temperature, and images were captured with a Zeiss AxioObserver Z1 inverted microscope.

To track the positioning of GFP MD4 B cells, spleens were fixed in 4% paraformaldehyde (PFA) for 2 hours at 4°C, washed with phosphate-buffered saline (PBS), submerged in 30% sucrose overnight, and embedded in optimal cutting temperature compound. Cryosections of 7 μm were dried for 1 hour at room temperature and rehydrated in PBS containing 0.1% fatty acid-free bovine serum albumin (BSA) for 10 min. A solution consisting of 1% NMS and NDS, 1:100 AF488-conjugated rabbit anti-GFP (Invitrogen, catalog no. A21311), 1:100 AF647-conjugated anti-mouse CD21/35, 1:100 biotin-conjugated anti-mouse CD4 (Biolegend, catalog no. 100404), and 1:300 goat anti-mouse IgD was used to label MD4 B cells, FDCs, endogenous CD4 T cells, and endogenous naïve B cells, respectively. These solutions were incubated with the slides overnight at 4°C. The slides were then washed in PBS and stained with Cy3-conjugated streptavidin (Jackson ImmunoResearch, catalog no. 016-160-084) and AMCA-conjugated donkey

anti-goat IgG for 1 hour at room temperature, and images were captured with a Zeiss AxioObserver Z1 inverted microscope.

Quantification of IF Images

Images of immunofluorescent stains of GFP MD4 B cell positioning were quantified using ImageJ (version 1.53). All images were captured at the same magnification using a Zeiss AxioObserver Z1 inverted microscope. Images were loaded into ImageJ and the freehand line tool was used to outline the T-B zone interface of a follicle. The total number of GFP MD4 B cells 20 μm on either side of the T-B interface was quantified. The number of GFP MD4 B cells inside the follicle was also quantified, and the proportion of GFP MD4 B cells at the T-B interface to GFP MD4 B cells in the follicle was calculated.

Cell Culture

CD4⁺ T cells from WT and *Ctsb*^{-/-} lymph nodes were enriched by negative selection using biotinylated antibodies against B220, CD8, CD11c, and Ter119, followed by streptavidin-conjugated beads to greater than 95% purity. Cells were plated in a 96-well plate at 5×10^6 cells per mL in RPMI medium 1640 plus 10% FCS at 37°C and rested or stimulated for 2 h with 10 ng/ml PMA and 1 $\mu\text{g/ml}$ ionomycin. To facilitate detection of surface exposed CD40L, the cells were incubated in the presence of 1 mg/mL anti-CD40L antibody as previously described (30, 31). To mimic CD40 deficiency, we plated CD4⁺ T cells from WT and *Ctsb*^{-/-} lymph nodes in a dilute culture of 0.5 mL at 5×10^5 cells per mL in 24-well plates and kept on ice or incubated at 37°C for 2 h.

Real-Time PCR Analysis

B6 and *Ctsb*^{-/-} spleens and lymph nodes were harvested and CD4⁺ T cells were enriched by negative selection using biotinylated antibodies against CD19, B220, CD8, CD11c, and Ter119, followed by streptavidin-conjugated beads to greater than 95% purity. Cell pellets were snap-frozen in liquid nitrogen, and RNA was prepared by using an RNeasy kit (Qiagen, Valencia, CA). Equivalent amounts of cDNA were used in quantitative PCR on an ABI 7300 sequence detection instrument (Applied Biosystems) by using primer sets with SYBR Green (Bio-Rad). Primer pairs were as follows (forward, F; reverse, R): hypoxanthine phosphoribosyltransferase (HPRT) F, AGGTTGCAAGCTTGCTGGT, and HPRT R, TGAAGTACTCATTATAGTCAAGGGCA; CD40 ligand F, GTGAGGAGATGAGAAGGCAA, and CD40 ligand R, CACTGTAGAACGGATGCTGC.

Flow Cytometry

Cells were stained for 20 min on ice in MACS buffer (2% FCS in PBS with 1 mM EDTA) at 0.5 to 1 × 10⁶ cells per well in 96-well round-bottom plates unless otherwise specified. The following monoclonal antibodies were used: B220–BV785 (BioLegend), ICAM1-biotin (BD) (followed by streptavidin–BV711 (Fisher)), CD45.2–PerCP-Cy5.5 (Tonbo), IgM^a–FITC (Fisher), CD40–PE (Fisher), CD23–PE-Cy7 (BioLegend), CD45.1–BV605 (BioLegend), CD40L–PE (BioLegend), and CD40L–biotin (eBioscience) (followed by streptavidin-A647 (Fisher)). Dead cells were excluded using Fixable Viability Dye eFluor780 (eBioscience no. 65-0865-18). All samples were run on a BD LSRII or BD FACSymphony A1 at 5,000 to 10,000 events per second. Flow cytometry data were analyzed using FlowJo (v10.8.1).

BAFF Staining

Staining for BAFF occupancy of BAFFR on B cells was as previously described (5). In brief, after FcR blocking, spleen cells were incubated with rabbit anti-mouse BAFF-ectodomain serum at a 1:1000 dilution, followed by 1:100 goat anti-rabbit-biotin with 2% NMS, normal rat serum (NRS), and normal goat serum (NGS), followed by streptavidin-A647 and antibodies to other markers. As a positive control, cells were incubated with recombinant BAFF prior to the antibody staining.

Statistical Analyses

Data were analyzed using unpaired Student's *t* test, and ordinary one-way ANOVA using Tukey's multiple comparisons test was performed when comparing one variable across multiple groups. Prism version 9 (GraphPad Software) was used for all statistical analyses and to generate plots. Each experiment was repeated at least three times, unless otherwise indicated in the figure legends. In summary graphs, points indicate individual samples and horizontal lines are means. All error bars represent SDs.

ACKNOWLEDGEMENTS

We thank Julie Zikherman for ML5 mice, Julie and Anthony Defranco for feedback on the project. M.Y.C. was supported by the BMS training grant; J.G.C. is an investigator of the Howard Hughes Medical Institute. This work was supported in part by NIH grant R01 AI45073.

DATA AVAILABILITY

All study data are included in this article and/or SI Appendix.

CHAPTER 3

Conclusions

CONCLUSIONS

Here we find that the elimination of peripheral B cells experiencing chronic signal-1 is partially dependent on extrinsic Ctsb activity. Since more than one source of Ctsb (hematopoietic or non-hematopoietic) was sufficient, we speculate that Ctsb was acting in an extracellular manner to reduce the availability of a factor (or factors) that augments the survival and proliferation of chronically BCR-engaged B cells. Ctsb activity in promoting B cell elimination was lost when CD4⁺ T cells, CD40L or CD40 was lacking. We suggest Ctsb acts in part by reducing signaling via the CD40L-CD40 axis during autoantigen-binding B cell-naïve CD4⁺ T cell encounter. The finding of increased generation of GC B cells in response to a model foreign antigen is also in accord with a possible increase in CD40L-CD40 signaling. However, we cannot exclude the possibility that Ctsb is acting via an independent pathway that cooperates with CD40L-CD40 or other T cell-derived signals. These data are summarized in the working model we propose below (**Fig. 3.1**). Overall, these findings identify a role for extracellular protease activity in establishing the extent of B cell tolerance to peripheral self-antigen and potentially the magnitude of the response to some foreign antigens.

A previous study showed that Ctsb could cleave CXCL13 in vitro and the truncated form was reported to be more potent in promoting B cell migration than the full-length form (16). Images were provided (without further quantification) suggesting that Ctsb-deficient mice have a loss of follicular structure and FDCs in lymph nodes. FDCs are maintained in lymphoid follicles via LTA1b2 signals provided by B cells in a partially CXCL13-dependent manner (22), making the observations in Ctsb-deficient mice internally consistent. In contrast to those observations, we failed to observe a defect in B cell follicular clustering in Ctsb-deficient mice, and the follicles contained intact FDC networks. The basis for this discrepancy between studies is

● CtsB produced by a diversity of stromal and hematopoietic cells

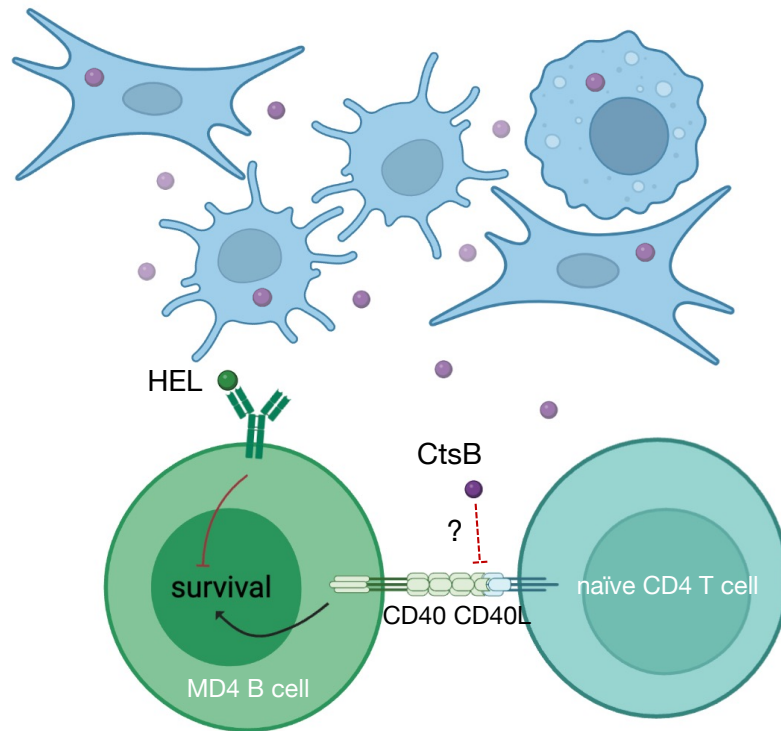


Figure 3.1 Model of the role of cathepsin B in augmenting survival of autoreactive B cells. Both stromal and hematopoietic sources of Ctsb are available to act extrinsically and extracellularly to reduce CD40-CD40L signaling, thereby restraining CD4⁺ T cell help to chronically antigen-engaged B cells.

unclear but might reflect different breeding histories of the mouse lines or differences in the microbiome between facilities. A side-by-side comparison of each strain of Ctsb-deficient mice will be needed in the future.

Although Ctsb was shown to be able to cleave CXCL13 in vitro, it was not shown that the enzyme has this activity in vivo (16). Since our anatomical findings suggest CXCL13 function does not depend on Ctsb, we have not examined whether CXCL13 is cleaved in vivo by Ctsb. Importantly, the influence of Ctsb on autoantigen-engaged B cell survival is unlikely to be via effects on CXCL13 as earlier studies have shown that CXCR5-deficient B cells that cannot

respond to CXCL13 undergo an equivalent extent of deletion as WT B cells in the HEL-MD4 model (23).

Ctsb acts on a wide range of intracellular and extracellular substrates (9, 10). While our study does not identify the molecule(s) that Ctsb acts on to restrain autoreactive B cell survival, our findings in CD4⁺ T cell-deficient, CD40L-blocked, and CD40-deficient systems point to actions that influence the CD40L-CD40 pathway. This possibility is also supported by the finding of increased ICAM1 and CD23 expression in chronically antigen-engaged B cells in Ctsb-deficient hosts as both these molecules are CD40-inducible (24, 25). The augmented proliferation in the case of B cells receiving chronic signal-1 and for MD4 B cells provided with cognate T cell help is also consistent with increased CD40 pathway activity. Our inability to detect significantly altered surface abundance of CD40L on CD4⁺ T cells or CD40 on B cells from Ctsb-deficient mice suggests Ctsb may affect this pathway in an indirect manner. However, it must be kept in mind that the activity of CD40L *in vivo* that augments autoreactive B cell survival likely reflects transient surface expression on naïve CD4⁺ T cells (8). Since we are not able to measure this low, transient surface CD40L, we cannot exclude that Ctsb, whether directly or indirectly, reduces the amount of CD40L available from naïve CD4⁺ T cells during interactions with chronically antigen-engaged B cells. In this regard, it is notable that a disintegrin and metalloprotease 10 (ADAM10) can promote reductions in surface CD40L (21). Work in cancer cell lines has indicated that Ctsb can promote release of soluble ADAM10 (27). These observations raise the possibility that Ctsb, by increasing soluble ADAM10 in tissues, reduces the amount of CD40L available at interfaces between T cells and B cells, a possibility that merits exploration. Alternatively, the effect of Ctsb is via a distinct pathway and this pathway can only show an influence on B cell survival and proliferation when the CD40L-CD40

pathway is intact; when this pathway is missing, the Ctsb-regulated pathway may be insufficient to have an influence. Future studies examining global gene expression changes in autoantigen-engaged B cells in WT versus Ctsb-deficient recipients at different time points may help determine the signaling pathway(s) most influenced by Ctsb.

Our study provides an example of a protease acting to influence the extent of tolerance induction in lymphoid tissues. Although less extensively tested, our work suggests this activity may also restrain the amount of help provided during responses to some foreign antigens. Interestingly, a recent report found that deficiency in prolidase, a cytosolic metallopeptidase, causes spontaneous T cell activation and lupus-like autoimmunity (28). It will be of interest in the future to determine if Ctsb deficiency predisposes to systemic autoimmune disease. Moreover, increases in protease activity are common at sites of inflammation and in tumors. It will be important in future studies to determine the extent to which immune checkpoints are reset in these sites due to proteolytic modulation of immune cell communication molecules.

REFERENCES

1. C. C. Goodnow, J. Sprent, B. Fazekas de St Groth, C. G. Vinuesa, Cellular and genetic mechanisms of self tolerance and autoimmunity. *Nature* **435**, 590-597 (2005).
2. C. C. Goodnow, J. Crosbie, H. Jorgensen, R. A. Brink, A. Basten, Induction of self-tolerance in mature peripheral B lymphocytes. *Nature* **342**, 385-391 (1989).
3. J. G. Cyster, S. B. Hartley, C. C. Goodnow, Competition for follicular niches excludes self-reactive cells from the recirculating B-cell repertoire. *Nature* **371**, 389-395 (1994).
4. J. G. Cyster, C. C. Goodnow, Antigen-induced exclusion from follicles and anergy are separate and complementary processes that influence peripheral B cell fate. *Immunity* **3**, 691-701 (1995).
5. R. Lesley *et al.*, Reduced competitiveness of autoantigen-engaged B cells due to increased dependence on BAFF. *Immunity* **20**, 441-453 (2004).
6. M. Thien *et al.*, Excess BAFF rescues self-reactive B cells from peripheral deletion and allows them to enter forbidden follicular and marginal zone niches. *Immunity* **20**, 785-798 (2004).
7. K. N. Schmidt, J. G. Cyster, Follicular exclusion and rapid elimination of hen egg lysozyme autoantigen-binding B cells are dependent on competitor B cells, but not on T cells. *J. Immunol.* **162**, 284-291 (1999).
8. R. Lesley, L. M. Kelly, Y. Xu, J. G. Cyster, Naive CD4 T cells constitutively express CD40L and augment autoreactive B cell survival. *Proc. Natl. Acad. Sci. U. S. A.* **103**, 10717-10722 (2006).
9. T. Yadati, T. Houben, A. Bitorina, R. Shiri-Sverdlov, The Ins and Outs of Cathepsins: Physiological Function and Role in Disease Management. *Cells* **9** (2020).

10. S. Roshy, B. F. Sloane, K. Moin, Pericellular cathepsin B and malignant progression. *Cancer Metastasis Rev.* **22**, 271-286 (2003).
11. K. Porter, Y. Lin, P. B. Liton, Cathepsin B is up-regulated and mediates extracellular matrix degradation in trabecular meshwork cells following phagocytic challenge. *PLoS One* **8**, e68668 (2013).
12. K. N. Balaji, N. Schaschke, W. Machleidt, M. Catalfamo, P. A. Henkart, Surface cathepsin B protects cytotoxic lymphocytes from self-destruction after degranulation. *J. Exp. Med.* **196**, 493-503 (2002).
13. S. M. Mariani, P. H. Krammer, Differential regulation of TRAIL and CD95 ligand in transformed cells of the T and B lymphocyte lineage. *Eur. J. Immunol.* **28**, 973-982 (1998).
14. M. Guo, P. A. Mathieu, B. Linebaugh, B. F. Sloane, J. J. Reiners, Jr., Phorbol ester activation of a proteolytic cascade capable of activating latent transforming growth factor-betaL a process initiated by the exocytosis of cathepsin B. *J. Biol. Chem.* **277**, 14829-14837 (2002).
15. L. Hasan *et al.*, Function of liver activation-regulated chemokine/CC chemokine ligand 20 is differently affected by cathepsin B and cathepsin D processing. *J. Immunol.* **176**, 6512-6522 (2006).
16. J. Cosgrove *et al.*, B cell zone reticular cell microenvironments shape CXCL13 gradient formation. *Nature communications* **11**, 3677 (2020).
17. L. Jackson, C. T. Cady, J. C. Cambier, TLR4-mediated signaling induces MMP9-dependent cleavage of B cell surface CD23. *J. Immunol.* **183**, 2585-2592 (2009).

18. F. Mackay, P. Schneider, P. Rennert, J. Browning, BAFF AND APRIL: a tutorial on B cell survival. *Annu. Rev. Immunol.* **21**, 231-264 (2003).
19. M. J. Yellin *et al.*, CD40 molecules induce down-modulation and endocytosis of T cell surface T cell-B cell activating molecule/CD40-L. Potential role in regulating helper effector function. *J. Immunol.* **152**, 598-608 (1994).
20. B. Ludewig *et al.*, Spontaneous apoptosis of dendritic cells is efficiently inhibited by TRAP (CD40-ligand) and TNF-alpha, but strongly enhanced by interleukin-10. *Eur. J. Immunol.* **25**, 1943-1950 (1995).
21. D. Yacoub *et al.*, CD154 is released from T-cells by a disintegrin and metalloproteinase domain-containing protein 10 (ADAM10) and ADAM17 in a CD40 protein-dependent manner. *J. Biol. Chem.* **288**, 36083-36093 (2013).
22. D. Paus *et al.*, Antigen recognition strength regulates the choice between extrafollicular plasma cell and germinal center B cell differentiation. *J. Exp. Med.* **203**, 1081-1091 (2006).
23. K. M. Ansel *et al.*, A chemokine driven positive feedback loop organizes lymphoid follicles. *Nature* **406**, 309-314 (2000).
24. E. H. Ekland, R. Forster, M. Lipp, J. G. Cyster, Requirements for follicular exclusion and competitive elimination of autoantigen binding B cells. *J. Immunol.* **172**, 4700-4708 (2004).
25. J. Banchereau *et al.*, The CD40 antigen and its ligand. *Annu. Rev. Immunol.* **12**, 881-922 (1994).

26. L. K. Busch, G. A. Bishop, The EBV transforming protein, latent membrane protein 1, mimics and cooperates with CD40 signaling in B lymphocytes. *J. Immunol.* **162**, 2555-2561 (1999).
27. F. C. Sigloch *et al.*, Proteomic analysis of silenced cathepsin B expression suggests non-proteolytic cathepsin B functionality. *Biochim. Biophys. Acta* **1863**, 2700-2709 (2016).
28. R. Hodgson *et al.*, Prolidase Deficiency Causes Spontaneous T Cell Activation and Lupus-Like Autoimmunity. *J. Immunol.* **210**, 547-557 (2023).
29. T. Yi, J. G. Cyster, EBI2-mediated bridging channel positioning supports splenic dendritic cell homeostasis and particulate antigen capture. *Elife* **2**, e00757 (2013).
30. Y. Koguchi, T. J. Thauland, M. K. Slifka, D. C. Parker, Preformed CD40 ligand exists in secretory lysosomes in effector and memory CD4⁺ T cells and is quickly expressed on the cell surface in an antigen-specific manner. *Blood* **110**, 2520-2527 (2007).
31. J. L. Gardell, D. C. Parker, CD40L is transferred to antigen-presenting B cells during delivery of T-cell help. *Eur. J. Immunol.* **47**, 41-50 (2017).

Publishing Agreement

It is the policy of the University to encourage open access and broad distribution of all theses, dissertations, and manuscripts. The Graduate Division will facilitate the distribution of UCSF theses, dissertations, and manuscripts to the UCSF Library for open access and distribution. UCSF will make such theses, dissertations, and manuscripts accessible to the public and will take reasonable steps to preserve these works in perpetuity.

I hereby grant the non-exclusive, perpetual right to The Regents of the University of California to reproduce, publicly display, distribute, preserve, and publish copies of my thesis, dissertation, or manuscript in any form or media, now existing or later derived, including access online for teaching, research, and public service purposes.

DocuSigned by:

Marissa Chou

92891B9B6B9043A...

Author Signature

3/17/2023

Date